

A rigorous and efficient approach to finding and quantifying symmetries in complex networks

Yong-Shang Long,¹ Zheng-Meng Zhai,¹ Ming Tang,^{1,2,*} Ying Liu,³ and Ying-Cheng Lai⁴

¹State Key Laboratory of Precision Spectroscopy and School of Physics and Electronic Science,
East China Normal University, Shanghai 200241, China

²Shanghai Key Laboratory of Multidimensional Information Processing,
East China Normal University, Shanghai 200241, China

³School of Computer Science, Southwest Petroleum University, Chengdu 610500, P. R. China

⁴School of Electrical, Computer and Energy Engineering, Arizona State University, Tempe, AZ 85287, USA

(Dated: August 6, 2021)

Symmetries are fundamental to dynamical processes in complex networks such as cluster synchronization, which have attracted a great deal of current research. Finding symmetric nodes in large complex networks, however, has relied on automorphism groups in algebraic group theory, which are solvable in quasipolynomial time. We articulate a conceptually appealing and computationally extremely efficient approach to finding and characterizing all symmetric nodes by introducing a structural position vector (SPV) for each and every node in the network. We prove mathematically that nodes with the identical SPV are symmetrical to each other. Utilizing six representative complex networks from the real world, we demonstrate that all symmetric nodes can be found in linear time, and the SPVs can not only characterize the similarity of nodes but also quantify the nodal influences in spreading dynamics on the network. Our SPV-based framework, in addition to being rigorously justified, provides a physically intuitive way to uncover, understand and exploit symmetric structures in complex networks.

PACS numbers: 05.45.Xt, 02.10.Ox

I. INTRODUCTION

Symmetries are ubiquitous in natural systems. In physics, the existence of a symmetry implies the conservation of a physical quantity and, as such, a great deal can be learned about the system without the need of analyzing the system details. The same principle has been applied to complex networks for identifying and understanding intricate dynamical phenomena such as cluster synchronization [1–5], which otherwise would be difficult to analyze. Given a complex network, a symmetry implies the existence of a group or a cluster of structurally completely equivalent nodes. When certain dynamical process occurs on the network, the nodes in a symmetric cluster, due to their complete equivalence, tend to be more readily synchronized among themselves than with nodes outside the cluster. A purely random network, such as the Erdős-Rényi network [6], typically has zero symmetry in the sense that the probability is zero for any two nodes to be equivalent in terms of their connection structure in the network. However, networks in the real world are not purely random but, in fact, they often possess a large number of symmetries [2, 7–9] that affect not only properties of the network such as spectrum, redundancy and robustness, but also the various dynamical processes on the network. For example, in the brain network, symmetries play an important role in the network dynamics such as remote synchronization and singularity [10, 11]. For network computations, symmetries can be exploited to coarse-grain and reduce the dimensionality of the network, merge symmetric nodes, and generate the so-called entropy graph of the original network [12] with re-

duced computational complexity [13, 14]. In complex networks, the mechanisms by which symmetries arise include replicative growth such as duplication [15], evolution from basic principles [9], and functional optimization [16].

In order to take advantage of the network symmetries, an essential task is to find all the symmetrical nodes. Existing methods are based on the algebraic group theory, such as dividing the equivalence class by backtracking search based on the coloring theory [17]. A commonly used algorithm is NAUTY - a set of procedures for efficiently determining the automorphism group of a vertex-colored graph [18]. A closely related problem is the classical graph isomorphism problem in theoretical computer science - to determine if two graphs are structurally identical or isomorphic. It was proved recently by Babai [19] that graph isomorphism is solvable in quasipolynomial time: $N^{P(\log N)}$ for a graph of N nodes, where $P(\cdot)$ is some polynomial. This means that, theoretically the graph isomorphism is almost efficiently solvable. While the existing algorithms are capable of finding the symmetric nodes, to quantify the symmetries associated with different nodes remains to be an open problem. In particular, in network science, a variety of centrality measures have been introduced to classify and characterize the importance of nodes, such as the degree, eigenvector centrality [20], betweenness [21], H-index [22], PageRank [23], k-core [24], etc., based on which concepts such as spectral coarse-grained networks have been developed [25, 26]. For a set of symmetric nodes, the values of these centrality measures are identical. In terms of the network symmetries, an important piece of knowledge that has been missing is to uncover a statistical measure to quantify the degree of symmetries among different nodes. The discovery of such a measure may also lead to more efficient algorithms for finding the symmetric nodes than the existing automorphism group based methods.

*Electronic address: tangminghan007@gmail.com

In the paper, we introduce an efficient statistical measure to characterize the network symmetries. By defining a structural position vector (SPV) for each and every node in the network, we exploit algebraic group theory to prove rigorously that having the same SPV for a set of nodes is sufficient to guarantee their symmetry. We demonstrate, using six large complex networks from the real world, that *all* the known symmetrical structures can be found accurately. In fact, since the computations required involve only a small number of multiplications between the adjacency matrix (that is typically sparse) and a vector, the symmetries can be found in linear time. We then propose and demonstrate an SPV-based index to describe the structural similarity among the nodes, which provides an effective algorithm for coarse-graining the network. We further articulate a centrality measure to quantify the nodal spreading influence - the role played by the nodes in the epidemic spreading dynamics, which is validated using real-world networks. Our SPV-based framework not only introduces a computationally extremely efficient method to find all the symmetric structures but also leads to a meaningful way to quantify the nodal symmetries, providing deeper insights into the symmetries of complex networks.

II. RESULTS

We first define SPVs and describe their relationship with nodal symmetries. We then use the finite-order SPVs to find the symmetric structures of six real-world networks and demonstrate how the SPVs can be used to describe the structural similarity of nodes. Finally, we propose an SPV-based centrality to quantify the nodal propagation influence.

A. SPVs and nodal symmetries

For nodes that are completely symmetrical to each other in the network, their structural positions are identical. First, we set an initial or the 0th-order structural position $l_i^0 = 1$ for each node in the network, where i is the nodal index. For all nodes in the network, their 0th-order structural positions can be represented by a vector: $\mathbf{L}^0 = [1, 1, \dots, 1]^T$. That is, initially, we disregard the edges and assume that all nodes have the same structural positions. To take into account the edges, we note that the structural position of a node is related to the structural positions of its n th order neighbors, which is determined by the n th power of the network adjacency matrix \mathcal{A}^n . Multiplying \mathbf{L}^0 from the left by \mathcal{A}^n , we get $\mathbf{L}^n = \mathcal{A}^n \cdot \mathbf{L}^0$, where \mathbf{L}^n ($n = 1, \dots, \infty$) is a vector containing information about the n th order structural positions of all nodes in the network, whose i th component is given by $L_i^n = \sum_{j=1}^N [A^n]_{ij} L_j^0$, which is the sum of the number of paths of length n to node i from all nodes in the network. Specifically, the 1st order structural position of a node is its degree and the ∞ th order is nothing but the eigenvector centrality of the node. Note that the vectors \mathbf{L}^n ($n = 1, \dots, \infty$) contain information about the structural positions of all nodes, but it is not the SPV that needs to be node-specific. To de-

fine the SPV for node i , we use the i th component in \mathbf{L}^n , for $n = 1, \dots, \infty$: $\mathbf{L}_i \equiv (L_i^1, L_i^2, \dots, L_i^\infty)$. While the vector \mathbf{L}_i is infinite-dimensional, for a finite network of size N , making the structural position vector \mathbf{L}_i N -dimensional suffices. We thus have $\mathbf{L}_i \equiv (L_i^1, L_i^2, \dots, L_i^N)$.

Making use of the algebraic group theory, we can prove rigorously that if the SPVs of nodes i and j are identical, i.e., $(L_i^1, L_i^2, \dots, L_i^N) = (L_j^1, L_j^2, \dots, L_j^N)$, then the two nodes are symmetrical to each other in the network. Details of the proof are presented in **Methods**.

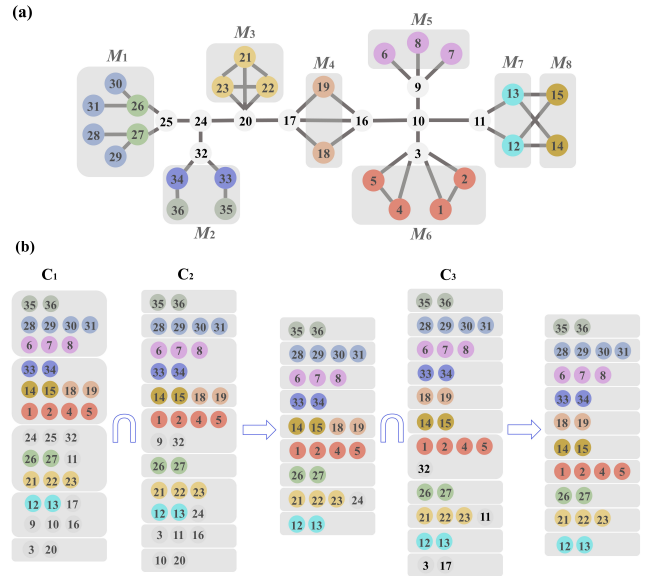


FIG. 1: Schematic representation of finding the symmetrical nodes using the SPVs. (a) A toy network containing eight symmetric motifs. (b) Nodal classification \mathbf{C}_n via the single n th-order vector \mathbf{L}^n , for $n = 1, 2, 3$, for each node in (a). The intersections of the nodal classification yield the symmetric nodes.

Figure 1 presents a simple example to illustrate how the symmetric nodes can be found using the SPVs. The toy network has eight symmetric motifs M_i ($i = 1, 2, \dots, 8$), as shown in Fig. 1(a). In motif M_1 , there are two sets of nodes that are symmetric to each other: $\{28, 29, 30, 31\}$ and $\{26, 27\}$. A set of symmetric nodes form an orbit, e.g., nodes 26 and 27. Motif M_1 thus consists of two orbits with two and four symmetric nodes, respectively, motif M_3 has one orbit of three symmetric nodes, and so on. We say that M_1 and M_3 are represented by the orbits $O_2 \xrightarrow{-2} O_4$ and O_3^* , respectively [**Supplementary Note (SN) 1**]. The orbital representations of the eight symmetric motifs in Fig. 1(a) and their corresponding geometric factors are listed in Table S1. The leftmost column in Fig. 1(b) is a diagram of five blocks determined according to the vector \mathbf{L}^1 , where all the nodes in a block have identical component values in \mathbf{L}^1 . Similarly, the columns under \mathbf{C}_2 and \mathbf{C}_3 have nine and 11 blocks, respectively. The middle column represents the set of intersection between the sets under \mathbf{C}_1 and \mathbf{C}_2 , which is done according to the criterion that all nodes in a block must have identical component values in both \mathbf{L}^1 and \mathbf{L}^2 , although the common

value in \mathbf{L}^1 may not equal that in \mathbf{L}^2 . The rightmost column in Fig. 1(b) consists of distinct blocks obtained through the interaction among the sets corresponding to \mathbf{C}_1 , \mathbf{C}_2 , and \mathbf{C}_3 , which already contain all the symmetric nodes of the network as specified in Fig. 1(a). This means that, for this toy network of 36 nodes, three iterations of the initial vector \mathbf{L}^0 already suffice to yield all the symmetric nodes.

We apply the principle to finding the symmetrical motifs in real-world networks. We consider six such networks: two information networks Odlis.net [27] and p2p-Gnutella [28], the social network Facebook [29], a cooperative network CA-GrQc [30], a biological network Yeast [31], and a voting network Wiki-Vote [32], whose structural properties are listed in Table I. Through the SPVs of the nodes, we succeed in finding all the symmetrical motifs in six representative real-world in linear time. The results are shown in Table S2 and Fig. S2.

B. Identification of symmetric nodes using SPVs

Theoretically, when calculating the SPVs of a network of size N , it is necessary to obtain all \mathbf{L}^n vectors for $n = 1, \dots, N$. However, if the network has a small diameter (as for many real-world networks [33]), \mathbf{L}^n tends to converge fast, typically requiring only a few iterations of $(\mathcal{A}^n \cdot \mathbf{L}^0)$. This means that, computationally, our method for finding the symmetric nodes can be extremely efficient. To quantify the computational efficiency, we define the following accuracy measure ρ to find the smallest n value, denoted as n^* , for which all symmetric structures in the network can be completely identified through the first n th-order SPVs:

$$\rho = \frac{\min\{U, Q\}}{\max\{U, Q\}} \frac{1}{U} \sum_{k=1}^U \frac{n_k}{N_k}, \quad (1)$$

where U is the number of non-trivial orbits in the symmetric structure of the network (see SN 1 for a definition of “orbits”) and Q is the number of nontrivial classes obtained through $\mathbf{C}_1 \cap \mathbf{C}_2 \cap \dots \cap \mathbf{C}_n$ [e.g., the distinct blocks in the rightmost column in Fig. 1(b)], where “nontrivial” means that there are at least 2 elements in the class. The quantity n_k ($k = 1, \dots, U$) is the number of nodes in the k th orbit of the network, and N_k is the number of nodes in the class (block) containing the k th orbit. By definition, we have $\rho \leq 1$. The larger the value of ρ is, the higher is the accuracy of the identified symmetric nodes. The perfect case $\rho = 1$ means that all symmetric nodes can be identified using the first n orders SPVs.

Figure 2 shows the accuracy measure ρ versus n for the six real-world networks listed in Tab. I. It can be seen that 100% accuracy as characterized by $\rho = 1$ is achieved for $n \geq 5$ for all six networks. For Facebook and Wiki-Vote network, this is achieved even for $n \geq 3$. The value of n^* is thus exceedingly small for all cases tested, indicating that all the symmetric nodes can be found extremely efficiently -in time that is only proportional to the size of the network (in linear time).

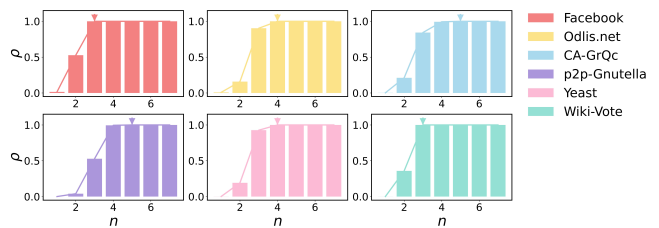


FIG. 2: Accuracy measure ρ of identifying all symmetric nodes versus the order- n SPVs for the six real-world networks in Tab. I. For Facebook and Wiki-Vote, the values of n^* , the minimum order required to have all symmetric nodes in the network correctly identified, are three. For Odlis.net and Yeast network, $n^* = 4$. For CA-GrQc and p2p-Gnutella networks, $n^* = 5$. The very small values of n^* across all the networks is strong indication that the SPV-based framework is computationally extremely efficient for finding all the symmetric nodes in large complex networks.

C. Quantifying nodal structure similarity based on SPVs

The similarity measure between two nodes based on their common neighbors has been widely used in problems such as link prediction and recommendation systems [34]. In general, two nodes with a similar connection structure often have similar values of multiple centrality measures such as degree, H-index, k-core, eigenvector centrality, and betweenness centrality, which is also important to coarse-graining networks and node influence identification. The use of a single centrality measure is usually not sufficient to describe the structural similarity between different nodes, as two nodes can have identical values for certain centrality but differ dramatically in other measures. (For example, nodes 10 and 12 in Fig. 1(a) have the same degree but their betweenness centrality values are quite different.) Symmetrical nodes are expected to have exactly the same SPV and centrality measures [13]. Intuitively, two nodes with similar (not equal) SPVs are structurally similar, so we define the following similarity index r , the Euclidean distance between the structural position vectors of nodes i and j :

$$r = \sqrt{\sum_{n=1}^N (\tilde{L}_i^n - \tilde{L}_j^n)^2}, \quad (2)$$

where \tilde{L}_i^n ($n = 1, 2, \dots, N$) is the n th component of the SPV of node i , normalized by the largest n th component value among all the nodes: $\tilde{L}_i^n = L_i^n / \max(L_1^n, L_2^n, \dots, L_N^n)$. A small value of r indicates a relatively high degree of similarity between the structures of nodes i and j . The results in Fig. 2 indicate that SPVs of size at most about five are needed to accurately identify all symmetric nodes in the six real-world networks. It thus suffices to use the following truncated SPV with six components: $\tilde{\mathbf{L}}_i^* \equiv (\tilde{L}_i^1, \tilde{L}_i^2, \dots, \tilde{L}_i^6)^T$, to calculate the similarity measure r .

As an application, we consider the problem of clustering nodes with similar structures. Our point is that the method based on the similarity index r defined in Eq. (2) performs better than many previously known methods. To demonstrate this, we use the k -mean algorithm to cluster the nodes in a

TABLE I: Structural properties of six real-world networks.

Networks	$ V $	$ E $	$\langle k \rangle$	$\langle d \rangle$	c	r
Facebook	4039	88234	43.69	3.69	0.606	0.064
Odlis.net	2909	16388	11.27	3.17	0.296	-0.173
CA-GrQc	4158	13422	6.46	6.05	0.557	0.639
p2p-Gnutella	6301	20779	6.60	4.64	0.011	0.035
Yeast	2224	6609	5.94	4.38	0.138	-0.105
Wiki-Vote	7066	100736	28.51	3.25	0.142	0.083

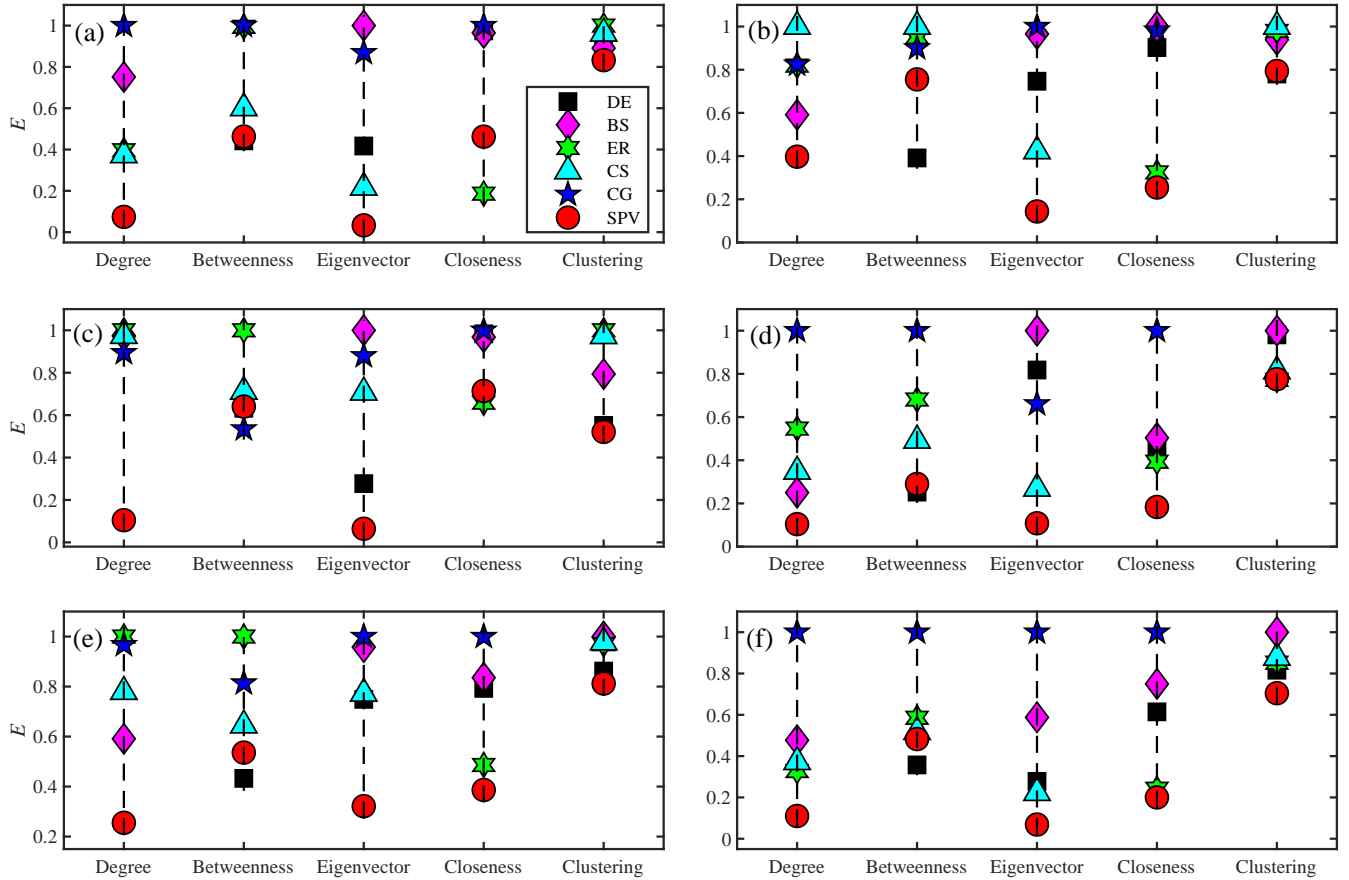


FIG. 3: Relative errors of node clustering by different clustering methods. (a-f): Respective results from six real-world networks: Facebook, Odlis.net, CA-GrQc, p2p-Gnutella, Yeast and Wiki-Vote. Black squares, pink diamonds, light green hexagon stars, cyan triangles, blue pentagrams and red circles represent the relative errors associated with the abscissa when clustering nodes based on degree (DE), betweenness (BS), eigenvector (ER), closeness centrality (CS), clustering centrality (CG) and structural position vector (SPV), respectively.

complex network into \tilde{N} classes. To verify the effect of clustering, we coarse-grain the network and use the properties of the center of each class to approximate the properties of nodes in this class. For a comparative analysis, we consider five clustering methods based on degree, betweenness, eigenvector centrality, closeness centrality, and clustering coefficient,

respectively. We define the coarse-grained error value E as

$$E = \sum_{c=1}^{\tilde{N}} \sum_{j=1}^{n_c} \sqrt{(z_{c_j} - Z_c)^2}, \quad (3)$$

where \tilde{N} is the number of clusters, n_c is the number of nodes in the c th cluster, z_{c_j} is a conventional statistical measure of node j in the c th cluster, and Z_c is the statistical measure of the center of the c th cluster. Given a network, we cluster all

the nodes using each of the six clustering methods. Each clustering method produces errors for the five conventional statistical measures. Except for the clustering method based on similarity index r , only the errors of the four statistical measures are calculated in the other five clustering methods. For example, if we coarse-grain the network using the nodal degree, we calculate the errors from betweenness, eigenvector centrality, closeness centrality, and clustering coefficient. (In this case, the error from the nodal degree must be minimum by definition, so including this error in the comparison is not meaningful.) We then normalize these coarse-grained error values to obtain the relative errors. Figure 3 shows, for the six real-world networks in Tab. I, the relative errors for the coarse-grained networks obtained from each of the six clustering methods, where the coarse-grained scale is $\tilde{N} = N(k)$, with $N(k)$ being the scale of coarse-grained network based on nodal degree. It can be seen that the relative node-clustering errors associated with three or four statistical measures are minimized when clustering nodes based on similarity index r . Especially the relative errors from degree, eigenvector centrality, and clustering coefficient are the smallest for all networks. In addition, the relative error of closeness centrality is the smallest for Odlis.net, p2p-Gnutella, Yeast, and Wiki-Vote when the coarse-grained network based on similarity index r . While in the remaining two networks, the relative error from closeness centrality can reach the second smallest although it is not the smallest. No conventional clustering method can generate node clustering as accurate as our similarity measure r , indicating that the SPVs can better describe the structural similarity of nodes than the conventional methods.

D. Quantifying role of nodes in propagation dynamics based on SPV

Propagation is a fundamental type of dynamical processes in real-world networks, with examples ranging from epidemic spreading in human social networks [35, 36] and diffusion of crisis in financial networks [37, 38] to cascading failures in power grids [39, 40] and signal transmission in neural networks [41, 42]. Measuring/quantifying the influence of nodes in propagation and identifying the nodes that play a critical role in the processes are issues with significant basic and applied values in network science. Conventionally, nodal centralities such as the degree, H-index and k-core are used for these purposes. The principle of coarse graining stipulates that nodes with the same degree, H-index or k-core have identical influences. Our result is that the SPVs provide an alternative and potentially more powerful way to measure the nodal influences in the propagation dynamics. This is based on the intuition that the more similar the structures of nodes, the closer are their influences.

Following our approach to quantifying nodal structure similarity, We cluster the network using the similarity index r and calculate the two-norm value b_i of the truncated SPVs $\tilde{\mathbf{L}}_i^*$ of the center of each class. This leads to the cluster centrality b_i based on the SPVs, which can be used to quantify the influence of nodes in this class. When the network is not clustered,

b_i is the SPV centrality.

To demonstrate the SPV-based quantification of nodal influences in propagation dynamics, we use the classic SIR (susceptible-infected-refractory) model. In the simulations, we set each node i is as the origin of the spreading dynamics and calculate the fraction R_i of the recovered nodes. We average over 5000 independent runs to obtain the mean R_i value that characterizes the propagation influence of node i . We thus have two sequences for all nodes in the network: the cluster centrality sequence (b_1, b_2, \dots, b_N) and the propagation influence sequence (R_1, R_2, \dots, R_N) , so their correlation can be calculated by using, e.g., the Kendall's correlation coefficient τ , where $-1 \leq \tau \leq 1$ (see SN 2 for a detailed definition). A large value of τ indicates a higher accuracy of the centrality in ranking the nodal influences. Fig. 4 shows, for the six real-world networks, Kendall's correlation coefficient between different cluster centralities and the propagation influence as \tilde{N} , the number of clusters increases. It can be seen that the cluster centralities are generally suitable for ranking the nodal influences. For example, for the network Odlis.net, Fig. 4(b) gives $\tau \geq 0.85$ and, for the Yeast network in Fig. 4(e), we have $\tau \geq 0.8$. Within a certain range, as the number of clusters increases, the correlation increases correspondingly. When the number of clusters is sufficiently large (e.g., $\tilde{N} \geq 50$), the correlation value plateaus. For comparison, we also calculate the correlation coefficient between the propagation influence sequence and each of the three conventional coarse-graining methods: degree, H-index, and k-core, where each method gives only a single value for each network. As shown in Fig. 4, for all six networks, the ranking performance of the SPV-based cluster centrality is consistently and significantly better than those of the three conventional methods in characterizing the nodal influences in epidemic spreading.

As the number of clusters exceeds about 50 ($\tilde{N} \geq 50$), the cluster centrality achieves a high accuracy in ranking the nodal influence. Note that, for $\tilde{N} = N$, the cluster centrality becomes the actual SPV centrality. Let $\text{SPV}(\tilde{N})$ denote the cluster centrality for the coarse-grained network of \tilde{N} clusters, where $\text{SPV} \equiv \text{SPV}(\tilde{N} = N)$. To systematically compare the nodal ranking performances of SPV and $\text{SPV}(\tilde{N})$ with those of the six conventional nodal ranking methods (i.e., those based on the degree, H-index, k-core, closeness, betweenness, and eigenvector centrality), we choose \tilde{N} to be the number of clusters obtained from the H-index. The results for the six real-world networks are listed in Tab. II, where the basic parameter β (the infection rate) associated with SIR dynamics is set to be $\beta = 1.2\beta_c$ with β_c being the propagation threshold value (SN 2). We see that SPV and $\text{SPV}(\tilde{N})$ have approximately the same accuracy that is generally higher than the accuracies of the conventional nodal ranking methods. There are a small number of exceptions. For example, in the p2p-Gnutella network, the eigenvector and closeness centralities have higher correlation with the propagation influence than that with the SPV-based methods. This is due to the fact that the network has no apparent local structures. Additional results for $\beta = 1.5\beta_c$ and $\beta = 2\beta_c$ can be found in Tables S3 and S4, respectively. We find that, except for

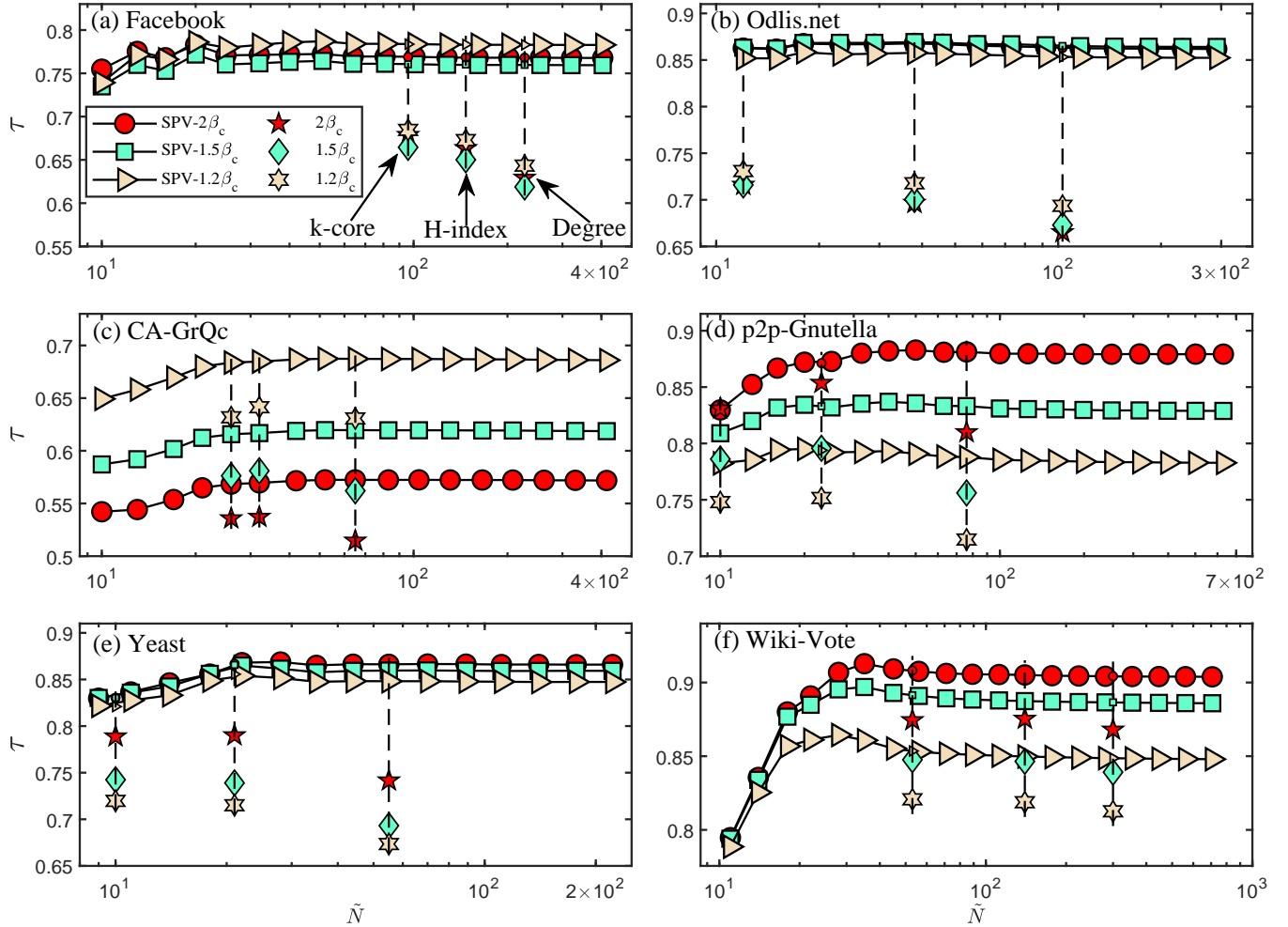


FIG. 4: Kendall's τ correlation coefficient for the six real-world networks. Shown is the τ value between the SPV-based cluster centrality and the nodal influence R versus \tilde{N} , the number of clusters in the SPV-based coarse-grained network for $0.001N \leq \tilde{N} \leq 0.1N$, with N being the size of the whole network. The light yellow triangles, light green squares, and red circles, respectively, represent the correlation coefficient τ between the SPV-based cluster centrality and the node influence R for infection rate $\beta = 1.2\beta_c$, $1.5\beta_c$, and $2\beta_c$ in the SIR dynamics. For comparison, the τ values between three conventional centralities (degree, H-index, and k-core) and R are shown. (For each conventional centrality, the corresponding coarse-grained network has a single value of \tilde{N} .) The light yellow six-pointed star, the light green diamond, and the red five-pointed star, respectively, represent the τ value between the three conventional centralities and R for $\beta = 1.2\beta_c$, $1.5\beta_c$, and $2\beta_c$.

the two networks p2p-Gnutella and CA-GrQc, the SPV-based cluster centralities have the best ranking performance. [In the CA-GrQc network, there is a high clustering coefficient c and assortativity r , indicating an core-periphery structure [43]. As a result, indices that reflect the importance of the core nodes (such as k-core, closeness centrality, eigenvector centrality) can better predict the spreading influence of nodes.]

In general, the influence of a node depends on the adjacency of different orders, corresponding to the components of each order in the SPV. The contribution of each order of adjacency is different [44]. Motivated by this, we further study the relative importance of each order component in the SPV to the influence of the node. Specifically, when clustering the nodes, we adjust the dimension of the truncated SPV and the weight of each order component. As shown in Figs. S2 and

S3, within a certain range, the more dimensions that the truncated SPV possesses, the better is the achieved ranking performance. Figures S4 and S5 show that, in a network with a small average path length, the importance of L^2 is larger than that of L^3 . In networks with a larger average path length, the conclusion is the opposite. (Details can be found in SN 3).

III. DISCUSSION

Symmetric structures are fundamental to dynamical processes on complex networks, and accurately identifying these structures is of great importance. While the existing, algebraic-group theory based methods can find all the symmetric nodes in the network in quasipolynomial time, these

TABLE II: Kendall's τ correlation coefficient between node influence R and eight indices for $\beta = 1.2\beta_c$.

Networks	Degree	H-index	k-core	Closeness	Betweenness	Eigenvector	SPV	SPV(\tilde{N})
Facebook	0.6434	0.6729	0.6846	0.4286	0.4331	0.6511	0.7869	0.7834
Odlis.net	0.6939	0.7178	0.7309	0.7801	0.5406	0.8307	0.8514	0.8577
CA-GrQc	0.6307	0.6413	0.6318	0.5806	0.3587	0.5965	0.6856	0.6847
p2p-Gnutella	0.7148	0.7516	0.7480	0.8309	0.6533	0.8452	0.7825	0.7939
Yeast	0.6734	0.7151	0.7197	0.8216	0.5646	0.8272	0.8476	0.8556
Wiki-Vote	0.8126	0.8188	0.8207	0.8257	0.7431	0.8508	0.8509	0.8498

methods do not yield a quantification or differentiation of the degree of symmetries. Two outstanding questions are: (1) does a method in linear time exist for finding all the symmetric structures of large complex networks? and (2) how to quantify the degree of nodal symmetries? This paper addresses both questions through the development of a unified framework. The fundamental concept that we articulate to accomplish this task is the nodal structural position vectors (SPVs). In particular, we define the SPV through the adjacency relationships in the network. Mathematically, by employing the algebraic group theory, we transform the relationship of equal SPVs into an eigenvector problem to rigorously prove that nodes with equal SPVs must be symmetrical. Utilizing real-world networks, we demonstrate that our SPV-based method allows all symmetric structures to be found with a small number of iterations of the SPV in computation time that is proportional to the network size. More importantly, our SPV-based framework enables the role of nodal symmetries in dynamical processes to be quantified and differentiated.

The similarity between two nodes based on common neighbors has been widely used in link prediction and recommendation systems. Since the symmetrical nodes have exactly the same structural characteristics, our SPV framework provides a natural way to define the structural similarity. In particular, defining a structural similarity index or centrality, we cluster the nodes in the network and find that the SPV-based clustering method is remarkably effective in coarse-graining the network in that it outperforms the previous clustering methods based on the traditional centralities such as the degree, eigenvector centrality, H-index, closeness and betweenness centralities. More importantly, from the standpoint of dynamical processes, our SPV-based clustering centrality can be used to measure and quantify the roles of nodes in propagation dynamics. Detailed calculation using six real-world networks indicates that, in most cases, the SPV-based centrality outperforms the conventional centralities by a large margin in predicting the nodal influences on propagation dynamics.

Taken together, our work provides a conceptually appealing and computationally extremely efficient framework to find symmetric nodes in large complex networks, totally bypassing the sophisticated steps in the conventional methods based on automorphism groups. The method also leads to a statistical characterization of nodal symmetries, with direct applications to coarse-graining of complex networks and cluster synchronization that may occur among remote nodes.

IV. METHODS

The main mathematical result of this paper is the theorem: *Nodes with equal SPVs must be symmetrical to each other.* Here we prove this theorem by using the algebraic group theory.

Mathematically, the existence of symmetric nodes in the network stipulates an automorphism π satisfying the property that $\{u, v\}$ is an edge in the network if and only if $\{\pi(u), \pi(v)\}$ is also an edge. All the automorphisms of a network constitute an automorphism group $G(\pi)$.

First, we prove two lemmas.

Lemma 1 The permutation π is an automorphism if and only if $\mathcal{P} \cdot \mathcal{A} = \mathcal{A} \cdot \mathcal{P}$, where \mathcal{A} , π and $\mathcal{P} = (p_{ij})$ are the adjacency matrix, permutation, and permutation matrix of the network, respectively. When nodes i and j have a permutation relation with each other: $v_i = \pi(v_j)$, the corresponding elements in the permutation matrix are $p_{ij} = p_{ji} = 1$, and all other elements are zero.

Proof: Assume $v_h = \pi(v_i)$, $v_k = \pi(v_j)$, then

$$\begin{cases} (\mathcal{P} \cdot \mathcal{A})_{hj} = \sum p_{hl} a_{lj} = a_{ij}, \\ (\mathcal{A} \cdot \mathcal{P})_{hj} = \sum a_{hl} p_{lj} = a_{hk}, \end{cases} \quad (4)$$

i.e., $\mathcal{P} \cdot \mathcal{A} = \mathcal{A} \cdot \mathcal{P}$ if and only if $a_{ij} = a_{hk}$. That is, the permutation π is an automorphism. ■

Lemma 2 If there is a permutation matrix \mathcal{P} such that $\mathcal{P} \cdot \mathbf{x} = \pm \mathbf{x}$, where \mathbf{x} is an eigenvector of the adjacency matrix of the network, then the permutation corresponding to \mathcal{P} is an automorphism.

Proof: Let $\mathcal{A} \cdot \mathbf{x} = \lambda \mathbf{x}$, where λ and \mathbf{x} are the eigenvalue and the associated eigenvector of the network adjacency matrix \mathcal{A} , respectively. Assume $\mathcal{P} \cdot \mathbf{x} = \pm \mathbf{x}$. Since the permutation matrix \mathcal{P} is derived from the identity matrix through a series of elementary transformations, \mathcal{P} is invertible. Left multiplying both sides of the characteristic equation $\mathcal{A} \cdot \mathbf{x} = \lambda \mathbf{x}$ by \mathcal{P} , we get $\mathcal{P} \cdot \mathcal{A} \cdot \mathbf{x} = \lambda \mathcal{P} \cdot \mathbf{x}$. With $\mathcal{P} \cdot \mathbf{x} = \pm \mathbf{x}$, we get

$$\mathcal{P} \cdot \mathcal{A} \cdot \mathbf{x} = \pm \lambda \mathbf{x} = \pm \mathcal{A} \cdot \mathbf{x} = \mathcal{A} \cdot \mathcal{P} \cdot \mathbf{x}, \quad (5)$$

which gives $(\mathcal{P} \cdot \mathcal{A} - \mathcal{A} \cdot \mathcal{P}) \cdot \mathbf{x} = 0$. Because \mathcal{A} is an $N \times N$ symmetric matrix, there must be N linearly independent eigenvectors, denoted as $\mathbf{x}_1, \mathbf{x}_2, \dots, \mathbf{x}_N$. The matrix $\mathcal{X} \equiv (\mathbf{x}_1, \mathbf{x}_2, \dots, \mathbf{x}_N)$ has full rank. We thus have $(\mathcal{P} \cdot \mathcal{A} - \mathcal{A} \cdot \mathcal{P}) \cdot \mathcal{X} = 0$. Expressing the matrix $(\mathcal{P} \cdot \mathcal{A} - \mathcal{A} \cdot \mathcal{P})$ in a row

form, we get

$$(\mathcal{P} \cdot \mathcal{A} - \mathcal{A} \cdot \mathcal{P}) \cdot \mathcal{X} = \begin{bmatrix} \phi_1 \\ \phi_2 \\ \vdots \\ \phi_N \end{bmatrix} \quad \mathcal{X} = \begin{bmatrix} 0 \\ 0 \\ \vdots \\ 0 \end{bmatrix}. \quad (6)$$

Since matrix \mathcal{X} has full rank, the equations $\phi_i \mathcal{X} = 0$ have trivial solutions only: $\phi_i = 0$. We thus have $\mathcal{P} \cdot \mathcal{A} = \mathcal{A} \cdot \mathcal{P}$. According to Lemma 1, the permutation corresponding to the permutation matrix \mathcal{P} is an automorphism. ■

Outline of proof of main theorem: Assume that the SPVs of the nodes x and y are equal: $\mathbf{L}_x^n = \mathbf{L}_y^n$ for $n = 1, 2, \dots, N$. Because \mathcal{A} is a symmetric matrix, it must have N linearly independent eigenvectors. The initial vector $\mathbf{L}^0 = (1, 1, \dots, 1)^T$ can then be linearly represented by the eigenvectors η_i for $i = 1, 2, \dots, N$: $\mathbf{L}^0 = \sum_{i=1}^N t_i \eta_i$. From $\mathbf{L}^n = \mathcal{A}^n \cdot \mathbf{L}^0$, we get

$$\begin{cases} \mathbf{L}^1 = \mathcal{A} \cdot \mathbf{L}^0 = \mathcal{A}(\sum_{i=1}^N t_i \eta_i) = \sum_{i=1}^N t_i \lambda_i \eta_i, \\ \mathbf{L}^2 = \mathcal{A}^2 \cdot \mathbf{L}^0 = \mathcal{A}^2(\sum_{i=1}^N t_i \eta_i) = \sum_{i=1}^N t_i \lambda_i^2 \eta_i, \\ \vdots \\ \mathbf{L}^N = \mathcal{A}^N \cdot \mathbf{L}^0 = \mathcal{A}^N(\sum_{i=1}^N t_i \eta_i) = \sum_{i=1}^N t_i \lambda_i^N \eta_i. \end{cases} \quad (7)$$

The equality $\mathbf{L}_x^n = \mathbf{L}_y^n$ for $n = 1, 2, \dots, N$ gives

$$\begin{cases} \sum_{i=1}^N t_i \lambda_i \eta_{i,x} = \sum_{i=1}^N t_i \lambda_i \eta_{i,y}, \\ \sum_{i=1}^N t_i \lambda_i^2 \eta_{i,x} = \sum_{i=1}^N t_i \lambda_i^2 \eta_{i,y}, \\ \vdots \\ \sum_{i=1}^N t_i \lambda_i^N \eta_{i,x} = \sum_{i=1}^N t_i \lambda_i^N \eta_{i,y}. \end{cases} \quad (8)$$

or

$$\begin{cases} \sum_{i=1}^N t_i \lambda_i (\eta_{i,x} - \eta_{i,y}) = 0, \\ \sum_{i=1}^N t_i \lambda_i^2 (\eta_{i,x} - \eta_{i,y}) = 0, \\ \vdots \\ \sum_{i=1}^N t_i \lambda_i^N (\eta_{i,x} - \eta_{i,y}) = 0. \end{cases} \quad (9)$$

The determinant of this set of linear equations in $(\eta_{i,x} - \eta_{i,y})$ is

$$C = \begin{vmatrix} t_1 \lambda_1 & t_2 \lambda_2 & \cdots & t_N \lambda_N \\ t_1 \lambda_1^2 & t_2 \lambda_2^2 & \cdots & t_N \lambda_N^2 \\ t_1 \lambda_1^3 & t_2 \lambda_2^3 & \cdots & t_N \lambda_N^3 \\ \vdots & \vdots & \ddots & \vdots \\ t_1 \lambda_1^N & t_2 \lambda_2^N & \cdots & t_N \lambda_N^N \end{vmatrix} = t_1 t_2 \cdots t_N \lambda_1 \lambda_2 \cdots \lambda_N \begin{vmatrix} 1 & 1 & \cdots & 1 \\ \lambda_1 & \lambda_2 & \cdots & \lambda_N \\ \lambda_1^2 & \lambda_2^2 & \cdots & \lambda_N^2 \\ \vdots & \vdots & \ddots & \vdots \\ \lambda_1^{N-1} & \lambda_2^{N-1} & \cdots & \lambda_N^{N-1} \end{vmatrix}. \quad (10)$$

which is the Vandermonde determinant. We have $C = t_1 t_2 \cdots t_N \lambda_1 \lambda_2 \cdots \lambda_N \prod_{1 \leq j < i \leq N} (\lambda_i - \lambda_j)$. If all eigenvalues of \mathcal{A} are simple, zero is not its eigenvalue and $t_i \neq 0$ for $i = 1, 2, \dots, N$, then we have $C \neq 0$. The only solution of $(\eta_{i,x} - \eta_{i,y})$ is zero, so $\eta_{i,x} = \eta_{i,y}$. The permutation of nodes x and y implies that all eigenvalues of \mathcal{A} must satisfy $\mathcal{P} \cdot \eta = \eta$. By Lemma 2, the permutation corresponding to the permutation matrix \mathcal{P} is an automorphism, so the nodes x and y are symmetrical to each other. ■

A more general and detailed proof is presented in **SN 4**.

Data Availability

All relevant data are available from the authors upon request.

Code Availability

All relevant computer codes are available from the authors upon request.

Acknowledgments

This work was supported by the National Natural Science Foundation of China under Grant Nos. 82161148012, 11975099, 11575041, and the Science and Technology Commission of Shanghai Municipality under Grant No. 14DZ2260800. The work at Arizona State University was supported by the Office of Naval Research through Grant No. N00014-21-1-2323.

Author Contributions

Y.-S.L., M.T., and Y.-C.L. designed research; Y.-S.L. performed research; Y.-S.L., Z.-M.Z., M.T., and Y.-C.L. contributed analytic tools; Y.-S.L., Z.-M.Z., M.T., and Y.L. analyzed data; Y.-S.L., M.T., Y.L., and Y.-C.L. wrote the paper.

Competing Interests

The authors declare no competing interests.

Correspondence

To whom correspondence should be addressed. E-mail: tangminghan007@gmail.com.

References

-
- [1] Stewart, I., Golubitsky, M. & Pivato, M. Symmetry groupoids and patterns of synchrony in coupled cell networks. *SIAM J. Appl. Dyn. Sys.* **2**, 609–646 (2003).
- [2] Pecora, L. M., Sorrentino, F., Hagerstrom, A. M., Murphy, T. E. & Roy, R. Cluster synchronization and isolated desynchronization in complex networks with symmetries. *Nat. Commun.* **5**, 1–8 (2014).
- [3] Sorrentino, F., Pecora, L. M., Hagerstrom, A. M., Murphy, T. E. & Roy, R. Complete characterization of the stability of cluster synchronization in complex dynamical networks. *Sci. Adv.* **2**, e1501737 (2016).
- [4] Sorrentino, F. & Pecora, L. Approximate cluster synchronization in networks with symmetries and parameter mismatches. *Chaos* **26**, 094823 (2016).
- [5] Della Rossa, F. *et al.* Symmetries and cluster synchronization in multilayer networks. *Nat. Commun.* **11**, 1–17 (2020).
- [6] Erdős, P. & Rényi, A. On random graphs I. *Publ. Math. Debrecen* **6**, 290–291 (1959).
- [7] MacArthur, B. D. & Sánchez-García, R. J. Spectral characteristics of network redundancy. *Phys. Rev. E* **80**, 026117 (2009).
- [8] MacArthur, B. D., Sánchez-García, R. J. & Anderson, J. W. Symmetry in complex networks. *Dis. Appl. Math.* **156**, 3525–3531 (2008).
- [9] Xiao, Y., Xiong, M., Wang, W. & Wang, H. Emergence of symmetry in complex networks. *Phys. Rev. E* **77**, 066108 (2008).
- [10] Nicosia, V., Valencia, M., Chavez, M., Díaz-Guilera, A. & Latora, V. Remote synchronization reveals network symmetries and functional modules. *Phys. Rev. Lett.* **110**, 174102 (2013).
- [11] Kang, L., Tian, C., Huo, S. & Liu, Z. A two-layered brain network model and its chimera state. *Sci. Rep.* **9**, 1–12 (2019).
- [12] Sorrentino, F., Siddique, A. B. & Pecora, L. M. Symmetries in the time-averaged dynamics of networks: Reducing unnecessary complexity through minimal network models. *Chaos* **29**, 011101 (2019).
- [13] Xiao, Y., MacArthur, B. D., Wang, H., Xiong, M. & Wang, W. Network quotients: Structural skeletons of complex systems. *Phys. Rev. E* **78**, 046102 (2008).
- [14] Sánchez-García, R. J. Exploiting symmetry in network analysis. *Commun. Phys.* **3**, 1–15 (2020).
- [15] Chung, F., Lu, L., Dewey, T. G. & Galas, D. J. Duplication models for biological networks. *J. Comp. Biol.* **10**, 677–687 (2003).
- [16] Nishikawa, T. & Motter, A. E. Network-complement transitions, symmetries, and cluster synchronization. *Chaos* **26**, 094818 (2016).
- [17] McKay, B. D. *Backtrack programming and the graph isomorphism problem*. Ph.D. thesis, University of Melbourne (1976).
- [18] McKay, B. D. Computing automorphisms and canonical labellings of graphs. In *Comb. Math.*, 223–232 (Springer, 1978).
- [19] Babai, L. Graph isomorphism in quasipolynomial time. In *Proceedings of the 48th Annual ACM Symposium on Theory of Computing (STOC'16)*, 684–697 (2016).
- [20] Bonacich, P. Power and centrality: A family of measures. *Ame. J. Sociol.* **92**, 1170–1182 (1987).
- [21] Freeman, L. C. A set of measures of centrality based on betweenness. *Sociometry* 35–41 (1977).
- [22] Hirsch, J. E. An index to quantify an individual’s scientific research output. *Proc. Nat. Acad. Sci. (USA)* **102**, 16569–16572 (2005).
- [23] Newman, M. E. J. *Networks: An Introduction* (Oxford University Press, Oxford, UK, 2010).
- [24] Dorogovtsev, S. N., Goltsev, A. V. & Mendes, J. F. F. K-core organization of complex networks. *Phys. Rev. Lett.* **96**, 040601 (2006).
- [25] Gfeller, D. & De Los Rios, P. Spectral coarse graining of complex networks. *Phys. Rev. Lett.* **99**, 038701 (2007).
- [26] Gfeller, D. & De Los Rios, P. Spectral coarse graining and synchronization in oscillator networks. *Phys. Rev. Lett.* **100**, 174104 (2008).
- [27] Reitz, J. M. Online dictionary for library and information science. *Danbury: Western Connecticut State University* (2014).
- [28] Ripeanu, M. & Foster, I. Mapping the gnutella network: Macroscopic properties of large-scale peer-to-peer systems. In *International Workshop on Peer-to-Peer Systems*, 85–93 (Springer, 2002).
- [29] McAuley, J. J. & Leskovec, J. Learning to discover social circles in ego networks. In *NIPS*, vol. 2012, 548–56 (Citeseer, 2012).
- [30] Leskovec, J., Kleinberg, J. & Faloutsos, C. Graph evolution: Densification and shrinking diameters. *ACM Trans. Knowledge Disc. Data (TKDD)* **1**, 2–es (2007).
- [31] Bu, D. *et al.* Topological structure analysis of the protein–protein interaction network in budding yeast. *Nuc. Acids Res.* **31**, 2443–2450 (2003).
- [32] Leskovec, J., Huttenlocher, D. & Kleinberg, J. Predicting positive and negative links in online social networks. In *Proceedings of the 19th International Conference on World Wide Web*, 641–650 (2010).
- [33] Xu, S., Wang, P. & Lü, J. Iterative neighbour-information gathering for ranking nodes in complex networks. *Sci. Rep.* **7**, 1–13 (2017).
- [34] Lü, L., Jin, C.-H. & Zhou, T. Similarity index based on local paths for link prediction of complex networks. *Phys. Rev. E* **80**, 046122 (2009).

- [35] Arunachalam, P. S. *et al.* Adjuvanting a subunit COVID-19 vaccine to induce protective immunity. *Nature* 1–10 (2021).
- [36] Feng, M., Cai, S.-M., Tang, M. & Lai, Y.-C. Equivalence and its invalidation between non-markovian and markovian spreading dynamics on complex networks. *Nature communications* **10**, 1–10 (2019).
- [37] Silva, T. C., Souza, S. R. S. & Tabak, B. M. Monitoring vulnerability and impact diffusion in financial networks. *J. Econ. Dyn. Cont.* **76**, 109–135 (2017).
- [38] Lin, Z.-H. *et al.* Non-markovian recovery makes complex networks more resilient against large-scale failures. *Nature communications* **11**, 1–10 (2020).
- [39] Yang, Y., Nishikawa, T. & Motter, A. E. Small vulnerable sets determine large network cascades in power grids. *Science* **358** (2017).
- [40] Schäfer, B., Witthaut, D., Timme, M. & Latora, V. Dynamically induced cascading failures in power grids. *Nat. Commun.* **9**, 1–13 (2018).
- [41] Avena-Koenigsberger, A., Misic, B. & Sporns, O. Communication dynamics in complex brain networks. *Nat. Rev. Neurosci.* **19**, 17 (2018).
- [42] Reza, A. G. & Rhee, J.-K. K. Nonlinear equalizer based on neural networks for pam-4 signal transmission using dml. *IEEE Photonics Technology Letters* **30**, 1416–1419 (2018).
- [43] Kojaku, S. & Masuda, N. Core-periphery structure requires something else in the network. *New J. Phys.* **20**, 043012 (2018).
- [44] Liu, Y., Tang, M., Zhou, T. & Do, Y. Identify influential spreaders in complex networks, the role of neighborhood. *Physica A* **452**, 289–298 (2016).

Supplementary Information for

A rigorous and efficient approach to finding and quantifying symmetries in complex networks

Yong-Shang Long, Zheng-Meng Zhai, Ming Tang*, Ying Liu, and Ying-Cheng Lai

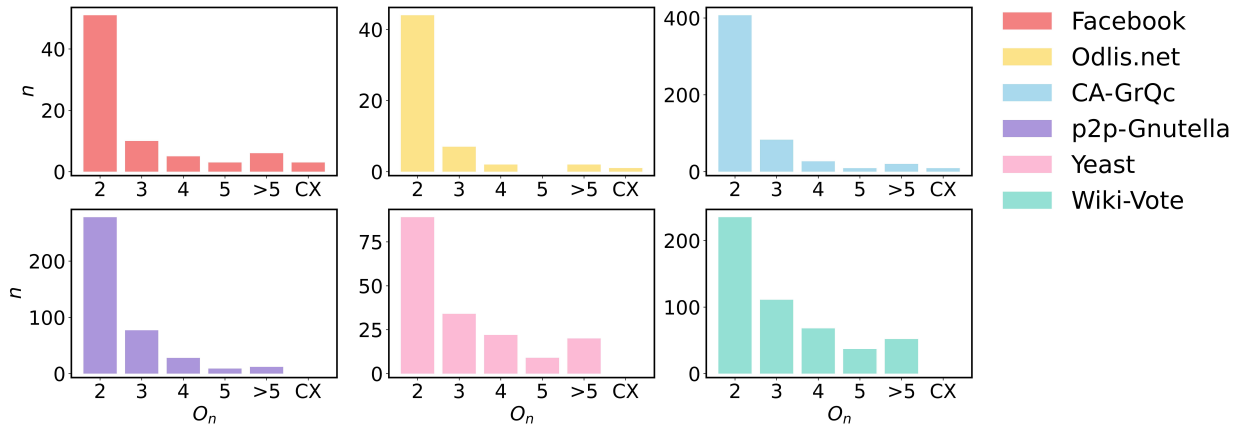
arXiv:2108.02597v1 [physics.soc-ph] 5 Aug 2021

Supplementary Note 1: Symmetry and automorphism groups

A network is a graph $G(V, E)$ with vertex set V and edge set E , where a pair of nodes are adjacent if there is an edge between them. An automorphism is a permutation of the vertices of the network, which preserves the adjacency. The combinations of a set of automorphisms form a group $\mathcal{G} = \text{Aut}(G)$ that describes the symmetries of the network [1]. A network with a nontrivial automorphism group is symmetric.

Consider the permutations of a set of N nodes $Y = v_1, v_2, \dots, v_N$. The support of a permutation p is the set of points that p moves: $\text{supp}(p) = \{v_i \in V(G) | p(v_i) \neq v_i\}$. Two sets of automorphisms, P and Q , are support-disjoint if every pair of automorphisms $p \in P$ and $q \in Q$ has disjoint support. Similarly, the automorphism subgroups G_p and G_q generated by P and Q are support-disjoint if P and Q are support-disjoint. The independent action of automorphism subgroups provides a way to factorize the automorphism groups of complex networks into “irreducible building blocks” [2]. In particular, let S be a set of generators of the automorphism groups $\text{Aut}(G)$. Suppose that we partition S into n support-disjoint subsets: $S = S_1 \cup S_2 \cdots S_n$, such that each S_i cannot itself be decomposed into smaller support-disjoint subsets. H_i is called the subgroup generated by S_i and every H_i commutes with all others. A direct product decomposition of the automorphism groups $\text{Aut}(G)$ is

$$\text{Aut}(G) = H_1 \times H_2 \times \cdots \times H_n. \quad (\text{S1})$$



Supplementary Figure S1. All symmetric motifs in six real-world networks. O_n is the number of nodes contained in the symmetric motifs, and “CX” denotes the complex symmetric motifs. The ordinate is the number of symmetric motifs.

The decomposition of automorphism group in Eq. (S1) is unique and irreducible [2]. The direct product factorization given in Eq. (S1) is the geometric decomposition of $\text{Aut}(G)$ and each factor H_i a geometric component. The induced subgraph on a set of vertices $X \subset V$ is the graph obtained by taking X and any edges whose end points are in X . The induced subgraph on the support of a geometric factor H_i is called the symmetric motif, denoted as M_H . A number of common symmetric motifs in the real-world networks are shown in Fig. 1(a). The orbital representation of the symmetric motifs therein and how the geometric factors of the automorphism group are related to different symmetric motifs are described in Supplementary Table S1. For every vertex $v \in V$, the set of vertices to which v maps under the action of the automorphism group $\mathcal{G} = \text{Aut}(G)$ is called a G -orbit of v , denoted as $\Delta(v)$. More formally, we have $\Delta(v) = \{g \cdot v \in V : g \in \text{Aut}(G)\}$. A symmetric motif generally consists of single or multiple orbits.

Supplementary Note 2: SIR model and Kendall’s τ correlation coefficient

SIR model. The standard SIR (susceptible-infected-recovered) model [4] has been widely used in simulating epidemic spreading and information propagation/diffusion dynamics. At each time step, an infected node makes contact

Supplementary Table S1. Orbital representation for the symmetric motifs and the corresponding geometric factors. The meanings of the symbols are as follows: O_α^* specifies that the orbit contains α nodes that are connected with each other; O_α means that the orbit contains α nodes and there is no connection between them; O_α^μ signifies that the orbit contains α nodes with μ edges between them; and $O_\alpha \xrightarrow{\gamma} O_{\alpha'}$ means that the symmetric motifs contain two orbits, and each node in the first orbit is connected to γ nodes in the second orbit. If $\gamma = \alpha'$, the symmetric motif is decomposed into two independent symmetric motifs, e.g., M_7 and M_8 in Fig. 1(a). The group of all permutation of n objects is denoted as S_n , C_n is the group of partial permutation of n objects, and \wr is the wreath product [3]. Supplementary Table S2 lists that there are mainly two symmetric motifs in the six real-world networks: O_α^* and O_α , which are the basic symmetric motifs. There are a few symmetrical motifs such as O_α^μ and $O_\alpha \xrightarrow{\gamma} O_{\alpha'}$, which are the complex symmetrical motifs.

Symmetric Motif	Orbital Representation	Geometric Factor
M_1	$O_2 \xrightarrow{2} O_4$	$S_2 \wr S_2$
M_2	$O_2 \xrightarrow{1} O_2$	$S_2 \wr S_1$ or S_2
M_3	O_3^*	S_3
M_4, M_7, M_8	O_2	S_2
M_5	O_3	S_3
M_6	O_4^2	C_4

Supplementary Table S2. Symmetric motifs of the six real networks in the main text

Network	Symmetric Motif
Facebook	$(O_2^*)^{33} + (O_2)^{18} + (O_3^*)^9 + O_3 + (O_4^*)^4 + O_4 + (O_5^*)^2 + O_5 + (O_7)^2 + O_9 + O_{11} + O_{13} + O_{14} + (O_4^2)^2 + O_6^3$
Odlis.net	$(O_2^*)^{14} + (O_2)^{30} + (O_3)^7 + (O_4)^2 + O_8 + O_{15} + (O_2 \xrightarrow{1} O_2^*)$
CA-GrQc	$(O_2^*)^{279} + (O_2)^{128} + (O_3^*)^{57} + (O_3)^{26} + (O_4^*)^{17} + (O_4)^{10} + (O_5^*)^7 + (O_5)^2 + (O_6^*)^4 + (O_6)^3 + O_7^* + O_8^* + O_9^* + O_{10}^* + O_{12}^* + O_{13}^* + O_{14}^* + O_{15}^* + O_{16}^* + O_{17}^* + O_{18}^* + O_{23}^* + O_{32}^* + (O_4^2)^7 + O_6^6 + O_{12}^{30}$
p2p-Gnutella	$O_2^* + (O_2)^{277} + (O_3)^{77} + (O_4)^{28} + (O_5)^9 + O_6 + (O_7)^3 + O_8 + O_9 + (O_{10})^4 + O_{26} + O_{32}$
Yeast	$(O_2^*)^2 + (O_2)^{87} + (O_3)^{34} + (O_4)^{22} + (O_5)^9 + (O_6)^9 + (O_7)^5 + (O_8)^3 + O_9 + (O_{10})^2$
Wiki-Vote	$(O_2)^{235} + (O_3)^{111} + (O_4)^{68} + (O_5)^{37} + (O_6)^{15} + (O_7)^{13} + (O_8)^5 + (O_9)^4 + (O_{10})^2 + (O_{12})^2 + (O_{13})^2 + O_{14} + O_{15} + O_{17} + O_{19} + O_{20} + O_{24} + O_{26} + O_{29} + O_{32}$

with its neighbors and each susceptible neighbor is infected with the probability β . The infected node enters into the state of recovery or removal with the probability λ . It is convenient to set $\lambda = 1$.

To quantify the spreading influence of node i , we initiate the spreading process with i being the infected seed and all other nodes being susceptible. The spreading process stops when there are no infected nodes. We record the fraction of recovered nodes R_i as the spreading influence of the seed node. According to the heterogeneous mean-field theory [5, 6], the epidemic threshold in the SIR model is given by $\beta_c = \langle k \rangle / (\langle k^2 \rangle - \langle k \rangle)$, where $\langle k \rangle$ is the average degree and $\langle k^2 \rangle$ is the second moment of the random degree variable. In our simulations, we set $\beta = 1.2\beta_c, 1.5\beta_c, 2\beta_c$. To eliminate the fluctuations of R_i , we average the results over 5000 independent runs.

Kendall's τ correlation coefficient. The Kendall's τ correlation coefficient is a widely used statistical measure for ranking the correlation. Consider two sequences associated with $|V|$ samples: $x = (x_1, x_2, \dots, x_{|V|})$ and $y = (y_1, y_2, \dots, y_{|V|})$. A pair of orders (x_i, x_j) and (y_i, y_j) are concordant if both $x_i > x_j$ and $y_i > y_j$ or if both $x_i < x_j$ and $y_i < y_j$, are discordant if $x_i > x_j$ and $y_i < y_j$ or if both $x_i < x_j$ and $y_i > y_j$. If $x_i = x_j$ or $y_i = y_j$, the pair is neither concordant nor discordant. As there are $|V|(|V| - 1)/2$ pairs of samples in total, the Kendall's τ correlation coefficient is defined as

$$\tau = 2(\delta^+ - \delta^-) / [|V|(|V| - 1)], \quad (S2)$$

where δ^+ and δ^- are the numbers of concordant and discordant pairs, respectively.

Supplementary Table S3.Kendall's τ correlation coefficient between node influence R and eight indices for $\beta = 1.5\beta_c$

Networks	Degree	H-index	k-core	Close-ness	Between-ness	Eigen-vector	SPV	SPV(\tilde{N})
Facebook	0.6187	0.6501	0.6645	0.4633	0.4219	0.6715	0.7633	0.7602
Odlis.net	0.6729	0.7004	0.7160	0.7915	0.5203	0.8505	0.8640	0.8693
CA-GrQc	0.5620	0.5810	0.5762	0.6284	0.3273	0.6477	0.6184	0.6168
p2p-Gnutella	0.7561	0.7957	0.7862	0.8813	0.6910	0.8228	0.8286	0.8330
Yeast	0.6932	0.7390	0.7424	0.8345	0.5762	0.8121	0.8599	0.8657
Wiki-Vote	0.8392	0.8465	0.8476	0.8543	0.7624	0.8853	0.8888	0.8874

Supplementary Table S4.Kendall's τ correlation coefficient between the nodal influence R and eight indices for $\beta = 2\beta_c$

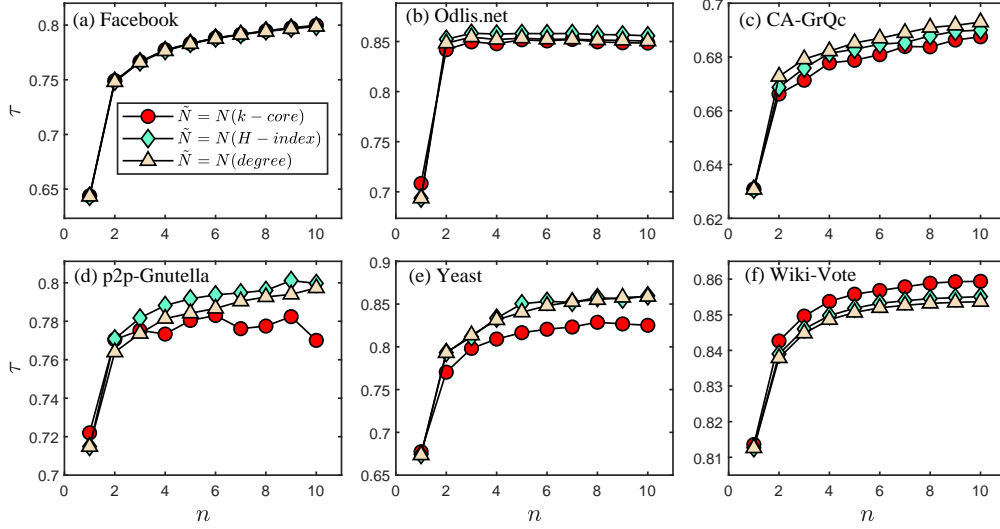
Networks	Degree	H-index	k-core	Close-ness	Between-ness	Eigen-vector	SPV	SPV(\tilde{N})
Facebook	0.6293	0.6635	0.6786	0.4955	0.4262	0.6579	0.7712	0.7685
Odlis.net	0.6651	0.6966	0.7160	0.7864	0.5101	0.8626	0.8632	0.8678
CA-GrQc	0.5146	0.5372	0.5358	0.6919	0.3172	0.6624	0.5718	0.5695
p2p-Gnutella	0.8099	0.8537	0.8309	0.9183	0.7385	0.7608	0.8794	0.8712
Yeast	0.7416	0.7900	0.7888	0.8152	0.6022	0.7689	0.8666	0.8669
Wiki-Vote	0.8680	0.8753	0.8744	0.8568	0.7789	0.8900	0.9038	0.9051

Supplementary Note 3: Impact of dimension of truncated SPV and its component weights on nodal propagation influence

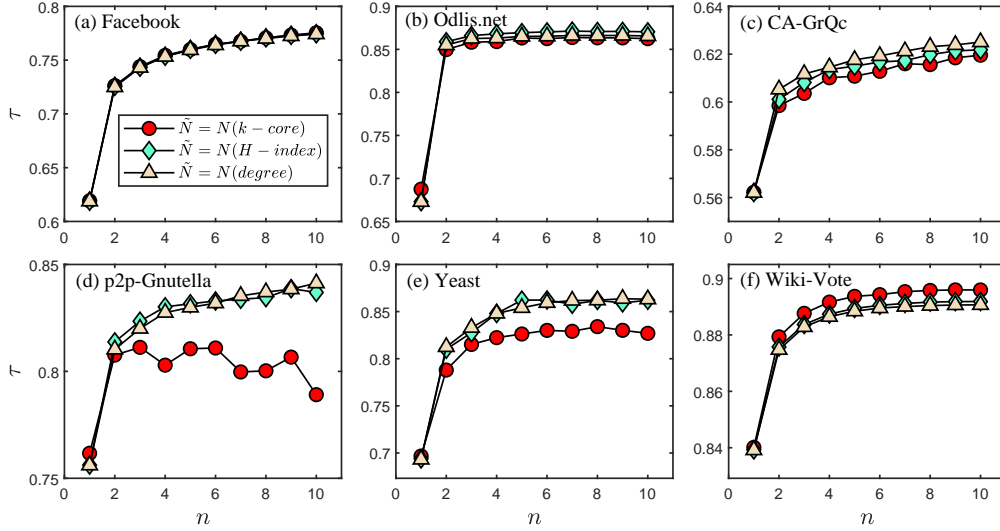
In the main text, we find that clustering nodes based on the first six orders of the truncated SPV $\tilde{\mathbf{L}}_i^*$ and the cluster centrality based on the SPV can well predict the influence of nodes on propagation dynamics. The influence of a node depends on its adjacency relationship at each order, corresponding to the order components in the truncated SPV. The contributions of the adjacency from different orders are different. Here we further study the relative importance of each order component in the SPV to the nodal propagation influence. We first set the dimension of $\tilde{\mathbf{L}}_i^*$ to be n : $\tilde{\mathbf{L}}_i^* = (L_i^1, L_i^2, \dots, L_i^n)$ for $n = 1, 2, \dots, 10$. The scale of the coarse-grained network is set to be $\tilde{N} = N(k)$, $N(\text{H-index})$, and $N(\text{k-core})$, respectively. To be representative, we consider two cases where the propagation rate is above the threshold: $\beta = 1.2\beta_c$ and $1.5\beta_c$. We then assign weights to different order components of $\tilde{\mathbf{L}}_i^*$: $\tilde{\mathbf{L}}_i^* = (w_1 L_i^1, w_2 L_i^2, \dots, w_n L_i^n)$.

Figures S2 and S3 show that, when using the SPV-based cluster centrality index to measure the influence of a node, the performance improves with the dimension of the SPV and then saturates. For example, if the SPV is one-dimensional, the only information it contains is the nodal degree, so the performance is relatively poor. However, a three-dimensional SPV can already predict the nodal influence well, but a higher dimensional SPV only leads to incremental improvement in the performance. In Figs. S2(d) and S3(d), for $\tilde{N} = N(k - \text{core})$, the performance curve is irregular, due mainly to the reason that the scale of the coarse-grained network is too small so the performance of the SPV based cluster centrality is not stable. In this case, increasing the dimension of the SPV does not improve the performance significantly. When the scale of the coarse-grained network is large, as the dimensionality increases, the level of classification becomes more detailed. In this case, the performance of cluster centrality tends to improve with the dimension before reaching a plateau.

We also study the relative importance of each component of the SPV to nodal propagation influence. Typically, the first three components of the SPV suffice to quantify the nodal influence. Generally, the nodal degree (the first-

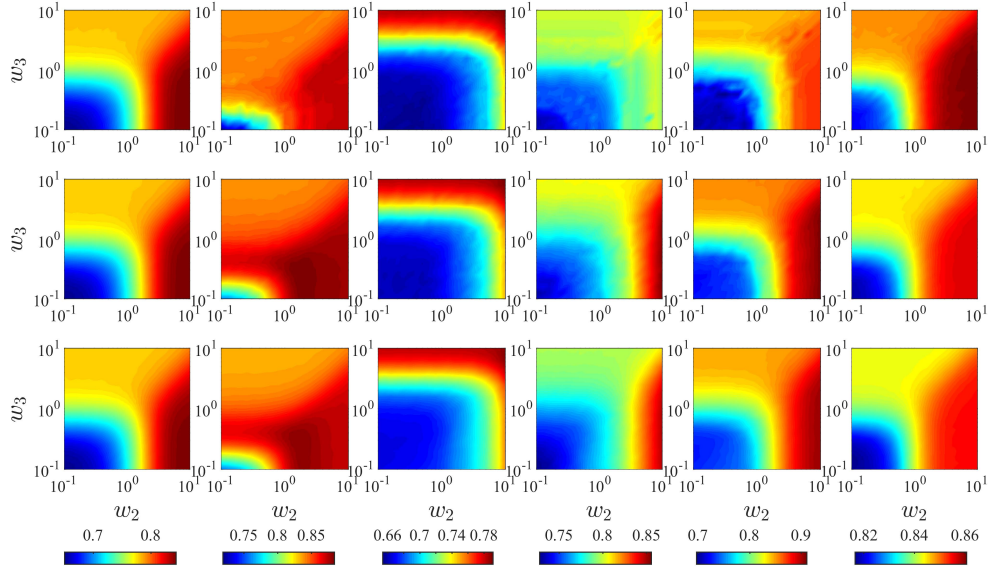


Supplementary Figure S2. Kendall' τ correlation coefficient between the SPV-based cluster centrality and nodal influence R as a function of the dimension n of the SPV for $\beta = 1.2\beta_c$.

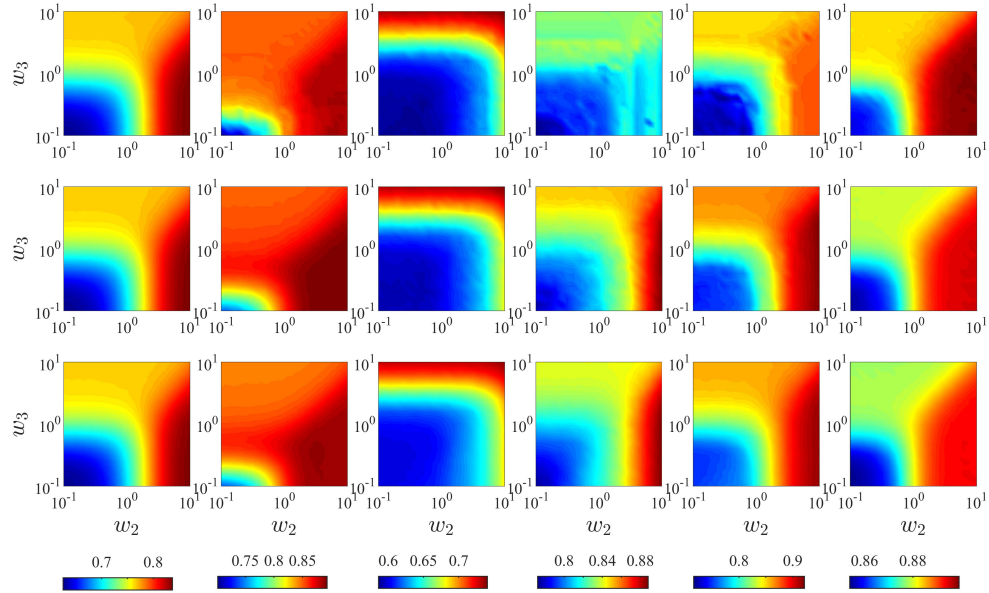


Supplementary Figure S3. Kendall' τ correlation coefficient between the SPV-based cluster centrality and nodal influence R as a function of the dimension n of the SPV for $\beta = 1.5\beta_c$.

order component of SPV) to some extent reflects the propagation influence of nodes. However, the extent to which the two-, three- and higher-dimensional structure of the SPV reflect the influence of nodes is worth elucidating. For this purpose, we study the relative importance of the two- and three-dimensional SPVs to nodal influence. In particular, we fix $w_1 = 1$ and adjust (w_2, w_3) in the range $0.1 \leq (w_2, w_3) \leq 10$. Figures S4 and S5 show that, except for the CA-GrQc network, when the SPV-based cluster centrality is used to quantify the nodal influence, the optimal region is $w_2 > 1, w_3 < 1$. We also find that increasing the weight of the second-order structural position has a larger impact on the nodal influence than increasing the weight of the third-order structural position. In the CA-GrQc network, the optimal area is in $w_3 > 1$, and increasing the weight of the third-order structural position has a larger impact on the ranking performance of cluster centrality. These results indicate that, when the average path length of the network is



Supplementary Figure S4. Effect of SPV component weights on nodal propagation influence. Shown is Kendall's τ correlation coefficient between the SPV-based cluster centrality and nodal influence R versus the weights of the second and third components of the truncated SPV (i.e., the second- and third-order structural positions), denoted as w_2 and w_3 , respectively, for $\beta = 1.2\beta_c$. From left to right, the networks in each column are Facebook, Odlis.net, CA-GrQc, p2p-Gnutella, Yeast, and Wiki-Vote. The scale of the coarse-grained network in each row from top to bottom is $\tilde{N} = N(k\text{-core})$, $N(H\text{-index})$ and $N(k)$.



Supplementary Figure S5. Effect of SPV component weights on nodal propagation influence. The legends are the same as those in Fig. S4 except that the value of parameter β is different: $\beta = 1.5\beta_c$.

small, the contribution of the second-order adjacency relationship to the nodal influence is greater than that of the third-order relationship. When the average path length of the network is large (e.g., the CA-GrQc network whose average path length is $\langle d \rangle = 6.05$), the contribution of the node's third-order adjacency relationship to the nodal influence is greater than that of the second-order relationship. (The average path lengths of the six real-world networks are listed

in table I in the main text).

Supplementary Note 4: General proof of main theorem: nodes with equal SPVs are symmetrical to each other

Following the outline of the proof of the main theorem in **Methods** in the main text, here we provide a general and detailed proof. If the SPVs of nodes x and y are equal, their corresponding eigencomponents satisfy the following equations:

$$\begin{cases} \sum_{i=1}^N c_i \lambda_i (\eta_{i,x} - \eta_{i,y}) = 0, \\ \sum_{i=1}^N c_i \lambda_i^2 (\eta_{i,x} - \eta_{i,y}) = 0, \\ \vdots \\ \sum_{i=1}^N c_i \lambda_i^N (\eta_{i,x} - \eta_{i,y}) = 0, \end{cases} \quad (\text{S3})$$

where some of the eigenvalues of the network adjacency matrix can be zero. Without loss of generality, we arbitrarily assume $\lambda_1 = 0$, $c_2 = 0$. In general, a large network has repeated eigenvalues. If the k th and the $(k+1)$ th eigenvalues are equal: $\lambda_k = \lambda_{k+1}$, Eq. (S3) becomes

$$\begin{cases} \sum_{i=3}^{k-1} c_i \lambda_i (\eta_{i,x} - \eta_{i,y}) + \lambda_k (c_k (\eta_{k,x} - \eta_{k,y}) + c_{k+1} (\eta_{k+1,x} - \eta_{k+1,y})) \\ + \sum_{i=k+2}^N c_i \lambda_i (\eta_{i,x} - \eta_{i,y}) = 0, \\ \sum_{i=3}^{k-1} c_i \lambda_i^2 (\eta_{i,x} - \eta_{i,y}) + \lambda_k^2 (c_k (\eta_{k,x} - \eta_{k,y}) + c_{k+1} (\eta_{k+1,x} - \eta_{k+1,y})) \\ + \sum_{i=k+2}^N c_i \lambda_i^2 (\eta_{i,x} - \eta_{i,y}) = 0, \\ \vdots \\ \sum_{i=3}^{k-1} c_i \lambda_i^N (\eta_{i,x} - \eta_{i,y}) + \lambda_k^N (c_k (\eta_{k,x} - \eta_{k,y}) + c_{k+1} (\eta_{k+1,x} - \eta_{k+1,y})) \\ + \sum_{i=k+2}^N c_i \lambda_i^N (\eta_{i,x} - \eta_{i,y}) = 0. \end{cases} \quad (\text{S4})$$

We take the first $(N-3)$ equations from Eq. (S4) to form a new set of equations. Regarding $\eta_{i,x} - \eta_{i,y}$ for $i = 3, 4, \dots, k-1, k+2, k+3, \dots, N$ and $c_k (\eta_{k,x} - \eta_{k,y}) + c_{k+1} (\eta_{k+1,x} - \eta_{k+1,y})$ for $i = k, k+1$ as unknown quantities, we have that the determinant of the coefficient of the new set of equations is

$$\begin{aligned} C' &= \begin{vmatrix} c_3 \lambda_3 & c_4 \lambda_4 & \cdots & c_{k-1} \lambda_{k-1} & \lambda_k & c_{k+2} \lambda_{k+2} & \cdots & c_N \lambda_N \\ c_3 \lambda_3^2 & c_4 \lambda_4^2 & \cdots & c_{k-1} \lambda_{k-1}^2 & \lambda_k^2 & c_{k+2} \lambda_{k+2}^2 & \cdots & c_N \lambda_N^2 \\ c_3 \lambda_3^3 & c_4 \lambda_4^3 & \cdots & c_{k-1} \lambda_{k-1}^3 & \lambda_k^3 & c_{k+2} \lambda_{k+2}^3 & \cdots & c_N \lambda_N^3 \\ \vdots & \vdots & \vdots & \vdots & \vdots & \vdots & \vdots & \vdots \\ c_3 \lambda_3^{N-3} & c_4 \lambda_4^{N-3} & \cdots & c_{k-1} \lambda_{k-1}^{N-3} & \lambda_k^{N-3} & c_{k+2} \lambda_{k+2}^{N-3} & \cdots & c_N \lambda_N^{N-3} \end{vmatrix} \\ &= c_3 c_4 \cdots c_{k-1} c_{k+2} \cdots c_N \lambda_3 \lambda_4 \cdots \lambda_k \lambda_{k+2} \cdots \lambda_N \\ &\cdot \begin{vmatrix} 1 & 1 & \cdots & 1 & 1 & 1 & \cdots & 1 \\ \lambda_3 & \lambda_4 & \cdots & \lambda_{k-1} & \lambda_k & \lambda_{k+2} & \cdots & \lambda_N \\ \lambda_3^2 & \lambda_4^2 & \cdots & \lambda_{k-1}^2 & \lambda_k^2 & \lambda_{k+2}^2 & \cdots & \lambda_N^2 \\ \vdots & \vdots & \vdots & \vdots & \vdots & \vdots & \vdots & \vdots \\ \lambda_3^{N-4} & \lambda_4^{N-4} & \cdots & \lambda_{k-1}^{N-4} & \lambda_k^{N-4} & \lambda_{k+2}^{N-4} & \cdots & \lambda_N^{N-4} \end{vmatrix} \end{aligned}$$

Because the multiplicity of eigenvalues has been eliminated, we have $\lambda_3 \neq \lambda_4 \neq \cdots \neq \lambda_k \neq \lambda_{k+2} \neq \cdots \neq \lambda_N$ and $c_i \neq 0$ for $i = 3, 4, \dots, k-1, k+2, k+3, \dots, N$, so $C' \neq 0$. The only solution of Eq. (S4) is trivial. In the eigenvectors representing \mathbf{L}^0 , insofar as the corresponding eigenvalues are not zero, the eigencomponents corresponding to nodes x and y are equal.

For nodes x and y with equal SPVs, we further analyze the relationship between their eigencomponents in the remaining eigenvectors. In particular, by transforming and simplifying the characteristic equations $\mathcal{A} \cdot \boldsymbol{\eta} = \lambda \boldsymbol{\eta}$, the eigencomponents corresponding to nodes x and y can be represented by the eigencomponents of any identical nodal

set S . We assume that the eigencomponents corresponding to nodes x and y are represented by the eigencomponents of node s_c and write

$$\varphi_0(\lambda_i)\eta_{i,x} = \varphi_1(\lambda_i)\eta_{i,s_c}, \quad (\text{S5})$$

$$\psi_0(\lambda_i)\eta_{i,y} = \psi_1(\lambda_i)\eta_{i,s_c}, \quad (\text{S6})$$

or

$$\frac{\varphi_0(\lambda_i)}{\psi_0(\lambda_i)}\eta_{i,x} = \frac{\varphi_1(\lambda_i)}{\psi_1(\lambda_i)}\eta_{i,y}. \quad (\text{S7})$$

Since $\varphi_0(\lambda_i)/\psi_0(\lambda_i)$ and $\varphi_1(\lambda_i)/\psi_1(\lambda_i)$ are polynomials in λ_i , we let $T_0(\lambda_i) \equiv \varphi_0(\lambda_i)/\psi_0(\lambda_i)$ and $T_1(\lambda_i) \equiv \varphi_1(\lambda_i)/\psi_1(\lambda_i)$. Equation (S7) becomes

$$T_0(\lambda_i)\eta_{i,x} = T_1(\lambda_i)\eta_{i,y}. \quad (\text{S8})$$

If the eigenvalue λ_i associated with the eigenvector used to represent \mathbf{L}^0 is non-zero, we have $\eta_{i,x} = \eta_{i,y}$ and

$$T_0(\lambda_i) = T_1(\lambda_i). \quad (\text{S9})$$

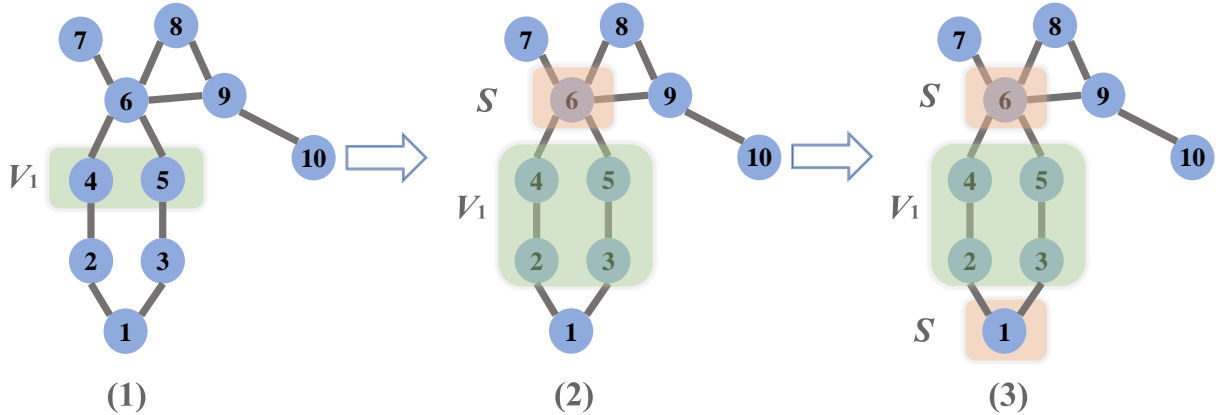
It is worth noting that the condition for Eq. (S9) to hold does not limit the value of λ_i (except zero), indicating that the equality $T_0(\lambda_i) = T_1(\lambda_i)$ does not depend on the value of λ_i . That is, the polynomials $T_0(\lambda_i)$ and $T_1(\lambda_i)$ are exactly the same. Substituting $\varphi_0(\lambda_i) = T_0(\lambda_i)\psi_0(\lambda_i)$ and $\varphi_1(\lambda_i) = T_1(\lambda_i)\psi_1(\lambda_i)$ into the Eq. (S5) gives

$$T_0(\lambda_i)\psi_0(\lambda_i)\eta_{i,x} = T_1(\lambda_i)\psi_1(\lambda_i)\eta_{i,s_c}, \quad (\text{S10})$$

or

$$\psi_0(\lambda_i)\eta_{i,x} = \psi_1(\lambda_i)\eta_{i,s_c}. \quad (\text{S11})$$

From Eqs. (S5) and (S11), we see that the eigencomponents corresponding to nodes x and y can be represented by the eigencomponents of any identical nodal set S , and the form of representation is exactly the same.



Supplementary Figure S6. Schematic illustration of determining nodal sets V_1 and S . (1) Take nodes 4 and 5 as an example. Let $V_1 = \{4, 5\}$. The characteristic equations of the two nodes are $\lambda_i\eta_{i,4} = \eta_{i,2} + \eta_{i,6}$ (e1) and $\lambda_i\eta_{i,5} = \eta_{i,3} + \eta_{i,6}$ (e2), respectively. (2) $S = \{6\}$. Substitute the characteristic equations of nodes 2 and 3 into (e1) and (e2), respectively, to get $(\lambda_i^2 - 1)\eta_{i,4} = \eta_{i,1} + \lambda_i\eta_{i,6}$, $(\lambda_i^2 - 1)\eta_{i,5} = \eta_{i,1} + \lambda_i\eta_{i,6}$, and $V_1 = \{2, 3, 4, 5\}$. (3) $S = \{1, 6\}$. The characteristic components of nodes 4 and 5 can be represented by the characteristic components of node set S , where $V_1 = \{2, 3, 4, 5\}$ and $S = \{1, 6\}$.

To find the identical node set S , we define the characteristic equation of node j as $\lambda_i\eta_{i,j} = \sum_{l \in \Lambda_j} \eta_{i,l}$, where $i = 1, 2, \dots, N$ and Λ_j is the set of neighboring nodes of j . That is, the eigencomponent of node j can be expressed by the eigencomponents of all its neighboring nodes. The process, as illustrated in Fig. S6, consists of the following four steps.

1. Analyze the characteristic equation $\lambda_i \eta_{i,x} = \sum_{j=1}^{k_x} \eta_{i,x_j}$ of node x with degree k_x , where x_j is a neighboring node of x . If all neighbors of x are removed, node x will be separated from the network. Denote $V_1 = \{x\}$.
2. Substitute the characteristic equation of a neighboring node x_1 of x into the characteristic equation of x so that the eigenvectors of node x are represented by the eigenvectors of its neighbors (excluding x_1) and the neighbors of x_1 . If the nodes used to represent the eigenvectors of x are removed, the local structure formed by nodes x and x_1 must be separated from the network. Denote $V_1 = \{x, x_1\}$.
3. Continue the iterative process in step 2 until the eigenvectors of node x is represented by the eigenvectors of nodal set S . If the characteristic equation of node m is used for iteration, then m is added to V_1 and $V_1 = \{x, x_i, \dots\}$. Remove nodal set S . The local structure $\text{local}_G(V_1, E_1)$ formed by V_1 is separated from the network, where E_1 is the set of internal edges of the node set V_1 .
4. Two possible situations can arise in determining nodal set S : two nodes may or may not have common neighboring nodes of different orders. The first case is where nodes x and y have common neighboring nodes. In this case, simplify the characteristic equations of nodes x and y according to step 2. If x and y have a common neighboring set $s_{1,xy}$, then $S = \{s_{1,xy}\}$. In this case, simplify the characteristic equations of x and y with the characteristic equations of non-common neighboring nodes and add these nodes to the set V_1 . If there is a second-order common neighboring set $s_{2,xy}$ between nodes x and y , add them to the set S to get $S = \{s_{1,xy}, s_{2,xy}\}$. Continue the process until the eigenvectors of x and y can be represented by the eigenvectors of S . The second case is where nodes x and y have no n th-order common neighbors. In this case, all neighbors of x constitute nodal set S .

Let the identical nodal set be $S = \{s_1, s_2, \dots, s_k\}$. Nodes of the network can then be divided into three sets: V_1 , S , and the remaining nodal set $V/\{V_1, S\}$. We perform elementary row transformation on matrix \mathcal{A} and divide it into blocks by row to get

$$\mathcal{A} \cdot \boldsymbol{\eta} = \begin{bmatrix} \mathcal{A}_1 \\ \mathcal{A}_2 \\ \mathcal{A}_3 \end{bmatrix} \cdot \boldsymbol{\eta} = \lambda \boldsymbol{\eta}, \quad (\text{S12})$$

where \mathcal{A}_1 , \mathcal{A}_2 and \mathcal{A}_3 are, respectively, $|V_1| \times N$, $|S| \times N$, and $|V/\{V_1, S\}| \times N$ adjacency matrices of the local structures formed by nodal sets V_1 , S , $V/\{V_1, S\}$ together with their neighbors. This analysis indicates that the eigenvectors of nodes x and y can be represented by the eigenvectors of nodal set $S = \{s_1, s_2, \dots, s_k\}$ through the characteristic equations $\mathcal{A}_1 \boldsymbol{\eta} = \lambda \boldsymbol{\eta}$. Since we have proved that the eigenvectors corresponding to x and y can be represented by the eigenvectors of any identical nodal set S , the representation is exactly the same. We thus have

$$f_0(\lambda_i) \eta_{i,x} = f_1(\lambda_i) \eta_{i,s_1} + f_2(\lambda_i) \eta_{i,s_2} + \dots + f_k(\lambda_i) \eta_{i,s_k}, \quad (\text{S13})$$

$$f_0(\lambda_i) \eta_{i,y} = f_1(\lambda_i) \eta_{i,s_1} + f_2(\lambda_i) \eta_{i,s_2} + \dots + f_k(\lambda_i) \eta_{i,s_k}. \quad (\text{S14})$$

If $f_0(\lambda_i) \neq 0$, then $\eta_{i,x} = \eta_{i,y}$. Permuting nodes x and y , we have that the eigenvectors associated with such eigenvalues satisfy $P\boldsymbol{\eta} = \boldsymbol{\eta}$.

We now discuss the case $f_0(\lambda_i) = 0$. It can be seen from Eqs. (S13) and (S14) that the eigenvectors of nodes x and y are free variables. In order to find the relationship between the eigenvectors of x and y , we further analyze the characteristic equation $\mathcal{A} \cdot \boldsymbol{\eta} = \lambda \boldsymbol{\eta}$. To do this, we move x and y out of nodal set V_1 and divide all nodes in the network into two sets: $V_1/\{x, y\}$ and $\{V/V_1, x, y\}$. The characteristic equation can be written as

$$\mathcal{A} \cdot \boldsymbol{\eta} = \begin{bmatrix} \mathcal{A}'_1 \\ \mathcal{A}'_2 \end{bmatrix} \cdot \boldsymbol{\eta} = \lambda \boldsymbol{\eta}, \quad (\text{S15})$$

where \mathcal{A}'_1 and \mathcal{A}'_2 are, respectively, $|V_1/\{x, y\}| \times N$ - and $|\{V/V_1, x, y\}| \times N$ -dimensional adjacency matrices of the local structures formed by nodal sets $V_1/\{x, y\}$ and $\{V/V_1, x, y\}$ as well as their neighbors. The eigenvectors of

$V_1/\{x, y\}$ can be represented by the eigencomponents of the set $\{x, y, S\}$ through the characteristic equation $\mathcal{A}'_1 \boldsymbol{\eta} = \lambda \boldsymbol{\eta}$. From Eqs. (S13) and (S14), the eigencomponents of x and y are related to the eigencomponents of nodal set S .

We are thus led to analyze the characteristic equation of any node $s_l \in S$: $\lambda_i \eta_{i,s_l} = \sum_{j \in \Lambda_{s_l}} \eta_{i,j}$, where $i = 1, 2, \dots, N$ and Λ_{s_l} is the set of neighbors of node s_l . We divide the neighbors of s_l into three parts: the first part is a subset of nodal set V_1 , the second part belongs to the set S , and the third part is contained in the set $V/\{V_1, S\}$. Since the eigencomponents of the nodes belonging to the set V_1 can be represented by the eigencomponents of the set $\{x, y, S\}$, the characteristic equation of node s_l can be written as

$$F_0(\lambda_i) \eta_{i,s_l} = G_0(\lambda_i) \eta_{i,x} + G_1(\lambda_i) \eta_{i,y} + \sum_{s_j \in S/s_l} F_j(\lambda_i) \eta_{i,s_j} + \sum_{j=1}^m H_j(\lambda_i) \eta_{i,r_j}, \quad (\text{S16})$$

where nodal set $R(r_1, r_2, \dots, r_m)$ are the neighbors of node s_l in the set $V/\{V_1, S\}$. Rearranging the terms, we get

$$F_0(\lambda_i) \eta_{i,s_l} - \sum_{s_j \in S/s_l} F_j(\lambda_i) \eta_{i,s_j} - \sum_{j=1}^m H_j(\lambda_i) \eta_{i,r_j} = G_0(\lambda_i) \eta_{i,x} + G_1(\lambda_i) \eta_{i,y}. \quad (\text{S17})$$

Let $E \equiv F_0(\lambda_i) \eta_{i,s_l} - \sum_{s_j \in S/s_l} F_j(\lambda_i) \eta_{i,s_j} - \sum_{j=1}^m H_j(\lambda_i) \eta_{i,r_j}$. Equation (S17) leads to

$$G_0(\lambda_i) \eta_{i,x} = E - G_1(\lambda_i) \eta_{i,y}, \quad (\text{S18})$$

$$G_1(\lambda_i) \eta_{i,y} = E - G_0(\lambda_i) \eta_{i,x}. \quad (\text{S19})$$

Multiplying both sides of Eqs. (S18) and (S19) by $G_0(\lambda_i)$ and $G_1(\lambda_i)$, respectively, and substituting Eqs. (S18) and (S19) into the resulting equations, we get

$$f_0(\lambda_i) G_1(\lambda_i) \eta_{i,y} = f_0(\lambda_i) E - (f_1(\lambda_i) \eta_{i,s_1} + f_2(\lambda_i) \eta_{i,s_2} + \dots + f_k(\lambda_i) \eta_{i,s_k}) G_0(\lambda_i), \quad (\text{S20})$$

$$f_0(\lambda_i) G_0(\lambda_i) \eta_{i,x} = f_0(\lambda_i) E - (f_1(\lambda_i) \eta_{i,s_1} + f_2(\lambda_i) \eta_{i,s_2} + \dots + f_k(\lambda_i) \eta_{i,s_k}) G_1(\lambda_i). \quad (\text{S21})$$

Since we have proved that the eigencomponents corresponding to nodes x and y can be represented by the eigencomponents of any identical nodal set, and the way of representation is exactly the same, we have $G_0(\lambda_i) = G_1(\lambda_i)$. Equation (S16) can be further simplified to

$$F_0(\lambda_i) \eta_{i,s_l} = G_0(\lambda_i) (\eta_{i,x} + \eta_{i,y}) + \sum_{s_j \in S/s_l} F_j(\lambda_i) \eta_{i,s_j} + \sum_{j=1}^m H_j(\lambda_i) \eta_{i,r_j}. \quad (\text{S22})$$

The above analysis indicates that Eqs. (S13) and (S14) are actually the consequence of the characteristic equations $\mathcal{A}_1 \boldsymbol{\eta} = \lambda \boldsymbol{\eta}$. As a result, the eigenvalue satisfying $f_0(\lambda_i) = 0$ is determined by the local structure $\text{local}_G(V_1, E_1)$ of nodal set V_1 only. Likewise, the eigenvector associated with this eigenvalue is related to the local structure $\text{local}_G(V_1, E_1)$ formed by V_1 only, so the eigencomponents of nodal set V/V_1 can be directly set to zero. Substituting the values of these components into the Eq. (S22), we have that the left side of this equation is zero, so are the second and third terms on the right side. We thus have

$$G_0(\lambda_i) (\eta_{i,x} + \eta_{i,y}) = 0 \text{ or } \eta_{i,x} + \eta_{i,y} = 0.$$

Apparently, for $f_0(\lambda_i) \neq 0$, the local structure $\text{local}_G(V_1, E_1)$ is not sufficient to determine this eigenvalue, so it must be related to the structure outside nodal set V_1 . The eigenvectors of matrix \mathcal{A} can be classified into two categories. The first category is $f_0(\lambda_i) \neq 0$, the eigenvectors are determined by the eigencomponents not only of nodal set V_1 but also of the set V/V_1 . The eigencomponents of nodes x and y satisfy $\eta_{i,x} = \eta_{i,y}$. In the second category defined by $f_0(\lambda_i) = 0$, the eigenvectors are related to the eigencomponents of nodal set V_1 only, and the eigencomponents of nodal set V/V_1 are all zero. In this case, the eigencomponents of x and y satisfy $\eta_{i,x} + \eta_{i,y} = 0$.

If there are nodes x' and y' with the same SPV in nodal set $V_1/\{x, y\}$, their characteristic components have similar properties to those of nodes x and y . In particular, for the first type of eigenvectors, the eigencomponents of x' and

y' satisfy $\eta_{i,x'} = \eta_{i,y'}$. For the second type, we have $\eta_{i,x'} + \eta_{i,y'} = 0$. If there is a node x'' in nodal set $V_1/\{x, y\}$, whose SPV is not equal to that of any other node in the set, then by using the characteristic equations $\mathcal{A}_1\boldsymbol{\eta} = \lambda\boldsymbol{\eta}$, the eigencomponents of x'' are represented by those of nodal set S . Similarly, consider the eigencomponents of node x'' for the two types of eigenvectors. In the first type, the value of the eigencomponent of x'' can be arbitrary. In the second type, according to Eq. (S16) or Eq. (S22), we have $\eta_{i,x''} = 0$. If the nodes $\{x, x'\}$ are permuted with $\{y, y'\}$, respectively, which have the same SPVs, all the eigenvectors of matrix \mathcal{A} satisfy $P\boldsymbol{\eta} = \boldsymbol{\eta}$ or $P\boldsymbol{\eta} = -\boldsymbol{\eta}$. If nodal set V_1 contains nodes x and y with the same SPV only, we permute the two nodes so that all the eigenvectors of matrix \mathcal{A} still satisfy $P\boldsymbol{\eta} = \boldsymbol{\eta}$ or $P\boldsymbol{\eta} = -\boldsymbol{\eta}$. In the following, we assume that nodal set V_1 contains only the nodes with equal SPVs.

When there are K ($K > 2$) nodes with the same SPV, we have $V_1 = \{q_1, q_2, \dots, q_K\}$. For the first type of eigenvectors, the eigencomponents of these K nodes satisfy $\eta_{i,q_1} = \eta_{i,q_2} = \dots = \eta_{i,q_K}$. Arbitrarily permuting these K nodes implies that the eigenvectors satisfy $P\boldsymbol{\eta} = \boldsymbol{\eta}$. For the second type of eigenvectors, the eigencomponents of the K nodes satisfy $\sum_{j=1}^K \eta_{i,q_j} = 0$. For $K = 2n$, where n is a positive integer greater than one, this gives $2n - 1$ linearly independent eigenvectors. From nodal set $\{q_1, q_2, \dots, q_K\}$, we pair the nodes arbitrarily. Without loss of generality, we write the pairing sequence as $(q_1, q_2), (q_3, q_4), \dots, (q_{2j-1}, q_{2j}), \dots, (q_{2n-1}, q_{2n})$. We then permute these paired nodes. We can prove that, with permutation under the above rule, all the eigenvectors of matrix \mathcal{A} satisfy $P\boldsymbol{\eta} = \pm\boldsymbol{\eta}$. In particular, the first type of eigenvectors satisfy $P\boldsymbol{\eta} = \pm\boldsymbol{\eta}$, so it is only necessary to prove that permuting the nodes can lead to $P\boldsymbol{\eta} = \pm\boldsymbol{\eta}$ for the second type of eigenvectors. We thus have that the number of eigenvectors of the second type is $2n - 1$. We then need to construct $2n - 1$ eigenvectors that satisfy $P\boldsymbol{\eta} = \pm\boldsymbol{\eta}$.

For the j th eigenvector ($j = 1, 2, \dots, n$), let $(\eta_{j,q_{2j-1}}, \eta_{j,q_{2j}}) = (1, -1)$ and the eigencomponents of the remaining $K - 2$ nodes in nodal set V_1 be zero. We obtain n K -dimensional vectors. Since, for the second type of eigenvectors, except for nodal set V_1 , the eigencomponents of the rest of the nodes are zero, we can simply expand them into $|V|$ -dimensional eigenvectors as

$$\begin{pmatrix} 1 & -1 & 0 & 0 & \cdots & 0 & 0 & 0 & 0 \\ 0 & 0 & 1 & -1 & \cdots & 0 & 0 & 0 & 0 \\ \vdots & \vdots & \vdots & \vdots & \vdots & \vdots & \vdots & \vdots & \vdots \\ 0 & 0 & 0 & 0 & \cdots & 1 & -1 & 0 & 0 \\ 0 & 0 & 0 & 0 & \cdots & 0 & 0 & 1 & -1 \end{pmatrix} \implies \begin{pmatrix} 1 & -1 & 0 & 0 & \cdots & 0 & 0 & 0 & 0 & 0 & 0 & \cdots & 0 & 0 \\ 0 & 0 & 1 & -1 & \cdots & 0 & 0 & 0 & 0 & 0 & 0 & \cdots & 0 & 0 \\ \vdots & \vdots & \vdots & \vdots & \vdots & \vdots & \vdots & \vdots & \vdots & \vdots & \vdots & \ddots & \vdots & \vdots \\ 0 & 0 & 0 & 0 & \cdots & 1 & -1 & 0 & 0 & 0 & 0 & \cdots & 0 & 0 \\ 0 & 0 & 0 & 0 & \cdots & 0 & 0 & 1 & -1 & 0 & 0 & \cdots & 0 & 0 \end{pmatrix}. \quad (\text{S23})$$

The n eigenvectors obtained by this method are linearly independent, which can be proved, as follows.

Proof: Denote each row of the matrix on the right side of (S23), from top to bottom, as $\eta_1, \eta_2, \dots, \eta_n$, respectively. There exist k_1, k_2, \dots, k_n such that $k_1\eta_1 + k_2\eta_2 + \dots + k_n\eta_n = 0$. We then have

$$(k_1, -k_1, k_2, -k_2, \dots, k_n, -k_n, 0, 0, \dots, 0, 0) = (0, 0, 0, 0, \dots, 0, 0, 0, 0, \dots, 0, 0). \quad (\text{S24})$$

We have $k_1 = k_2 = \dots = k_n = 0$, indicating that the group of vectors $\eta_1, \eta_2, \dots, \eta_n$ are linearly independent, which are n linearly independent eigenvectors that satisfy $P\boldsymbol{\eta} = -\boldsymbol{\eta}$. ■

We search for $n - 1$ linearly independent eigenvectors that satisfy $P\boldsymbol{\eta} = \boldsymbol{\eta}$, which are also linearly independent of the n eigenvectors found above. For the j th eigenvector ($j = 1, 2, \dots, n$), let $(\eta_{j,q_1}, \eta_{j,q_2}) = (1, 1)$, $(\eta_{j,q_{2j-1}}, \eta_{j,q_{2j}}) = (-1, -1)$ and the eigencomponents of the remaining $K - 4$ nodes in nodal set V_1 be zero. This leads to $n - 1$ K -dimensional vectors. Similarly, we expand them into $|V|$ -dimensional eigenvectors, as in formula (S23). Apparently, the eigenvectors so constructed satisfy $P\boldsymbol{\eta} = \boldsymbol{\eta}$. Here we prove that the newly constructed $n - 1$ eigenvectors are linearly independent of each other and are also linearly independent of the n eigenvectors found above.

Proof: The matrix composed of the newly constructed $n - 1$ vectors is

$$\begin{pmatrix} 1 & 1 & -1 & -1 & 0 & 0 & \cdots & 0 & 0 & 0 & 0 & \left| \begin{array}{ccc} 0 & 0 & \cdots & 0 & 0 \\ 0 & 0 & \cdots & 0 & 0 \\ \vdots & \vdots & \ddots & \vdots & \vdots \end{array} \right. \\ 1 & 1 & 0 & 0 & -1 & -1 & \cdots & 0 & 0 & 0 & 0 & \left| \begin{array}{ccc} 0 & 0 & \cdots & 0 & 0 \\ 0 & 0 & \cdots & 0 & 0 \\ \vdots & \vdots & \ddots & \vdots & \vdots \end{array} \right. \\ \vdots & \vdots & \vdots & \vdots & \vdots & \vdots & \ddots & \vdots & \vdots & \vdots & \vdots & \left| \begin{array}{ccc} \vdots & \vdots & \ddots & \vdots & \vdots \\ \vdots & \vdots & \ddots & \vdots & \vdots \\ \vdots & \vdots & \ddots & \vdots & \vdots \end{array} \right. \\ 1 & 1 & 0 & 0 & 0 & 0 & \cdots & -1 & -1 & 0 & 0 & \left| \begin{array}{ccc} 0 & 0 & \cdots & 0 & 0 \\ 0 & 0 & \cdots & 0 & 0 \\ \vdots & \vdots & \ddots & \vdots & \vdots \end{array} \right. \\ 1 & 1 & 0 & 0 & 0 & 0 & \cdots & 0 & 0 & -1 & -1 & \left| \begin{array}{ccc} 0 & 0 & \cdots & 0 & 0 \\ 0 & 0 & \cdots & 0 & 0 \\ \vdots & \vdots & \ddots & \vdots & \vdots \end{array} \right. \end{pmatrix}. \quad (\text{S25})$$

Denote each row of the matrix as $\eta_{n+1}, \eta_{n+2}, \dots, \eta_{2n-1}$, respectively, from top to bottom. There exist $k_1, k_2, \dots, k_{2n-1}$ such that $k_1\eta_1 + k_2\eta_2 + \dots + k_{2n-1}\eta_{2n-1} = 0$. We have

$$\begin{cases} k_1 + \sum_{l=n+1}^{2n-1} k_l = 0, \\ -k_1 + \sum_{l=n+1}^{2n-1} k_l = 0, \end{cases} \quad (\text{S26})$$

and

$$\begin{cases} k_{j+1} - k_{n+j} = 0 \\ -k_{j+1} - k_{n+j} = 0 \end{cases}, j = 1, 2, \dots, n-1. \quad (\text{S27})$$

From Eqs. (S26) and (S27), we have $k_1 = k_2 = \dots = k_{2n-1} = 0$, which means that the group of vectors $\eta_1, \eta_2, \dots, \eta_{2n-1}$ are linearly independent of each other, leading to $2n - 1$ linearly independent eigenvectors. Among them, n eigenvectors satisfy $P\eta = -\eta$ and $n - 1$ eigenvectors satisfy $P\eta = \eta$. ■

For $K = 2n + 1$, where n is a positive integer, there are $2n$ linearly independent eigenvectors. Similarly, we perform node pairing and permutation to construct the $2n$ eigenvectors. The first $2n - 1$ eigenvectors are constructed in the same way as for $K = 2n$, and the last eigenvector is $\eta_{2n} = (1, 1, \dots, 1, 1, -2n, 0, 0 \dots, 0, 0)$. The eigenvector η_{2n} is then linearly independent of the above $2n - 1$ eigenvectors and we have $P\eta = \eta$.

To summarize this Supplementary Note, we have that, according to the permutation method explained, all eigenvectors of the network satisfy $P\eta = \pm\eta$. Since we pair nodes arbitrarily, permuting any two nodes can make all the eigenvalues satisfy $P\eta = \pm\eta$. According to Lemma 2 in the main text, the permutation corresponding to the permutation matrix P is an automorphism. That is, nodes with identical SPVs are symmetric to each other.

Supplementary References

- [1] Bollobás, B. *Modern Graph Theory*, vol. 184 (Springer Science & Business Media, 2013).
- [2] MacArthur, B. D., Sánchez-García, R. J. & Anderson, J. W. Symmetry in complex networks. *Dis. Appl. Math.* **156**, 3525–3531 (2008).
- [3] Rotman, J. J. *An Introduction to the Theory of Groups*, vol. 148 (Springer Science & Business Media, 2012).
- [4] Pastor-Satorras, R., Castellano, C., Van Mieghem, P. & Vespignani, A. Epidemic processes in complex networks. *Rev. Mod. Phys.* **87**, 925 (2015).
- [5] Newman, M. E. Spread of epidemic disease on networks. *Phys. Rev. E* **66**, 016128 (2002).
- [6] Castellano, C. & Pastor-Satorras, R. Thresholds for epidemic spreading in networks. *Phys. Rev. Lett.* **105**, 218701 (2010).